BSU International Journal of Humanities and Social Science
Available Online: http://buijhs.journals.ekb.eg/
Online ISSN: 2314-8810 Print ISSN: 2314-8802

GIS-Based Bivariate Statistical Model Prediction of Groundwater Potential Mapping for Sustainable Developments in Suez Governorate, Egypt

Dr.Mohamed Sayed Kamel
Lecturer in Geography and GIS Department, Faculty of Arts, Suez University
Dr. Emad Abdel fattah Saleh Hafez
Lecturer in Geography and GIS Department, Faculty of Arts, Beni Suef University.

ABSTRACT

One of the primary challenges for sustainable development in semi-arid regions like Egypt, is the scarcity of freshwater, making it critical to assess groundwater potential. The purpose of the current study is to predict spatially potential groundwater zones in Suez Governorate (SG), Egypt using (relative frequency prediction rate) integration and Shannon entropy (SE) bivariate statistical models. Sixteen causal factors affecting groundwater instances were assessed in terms of geo-environmental. The results obtained from the current study revealed that these two models can be effectively working for spatial prediction modeling. Furthermore, the RF-PR model results have shown that most paramount factors in groundwater instances in study region were observed in soil units, depth to water table, LU/LC and drainage density whereas SE model reflects LU/LC, lithology, Distance to stream, soil units, and depth to water table respectively. Following by validation analysis of AUCs for both relative frequency-prediction rate and Shannon's models are 0.749 and 0.745, correspondingly, representing that RF-PR outperforms the Shannon's. Finally, groundwater potential zones prediction maps (GPZPm) obtained from both models were categorized into five classes. Current research results are useful for multi-criteria decision makers such as water resources authorities and decision architects to broadly assess the groundwater investigation for future planning.

Keywords
relative frequency; predictor rate; Shannon entropy; multi-criteria decision makers; SDGs.

1. Introduction

Groundwater represents one of the most important resources of natural stocked in underground strata in critical regions of the earth's crust (Fitts, 2012). Human survival, sustainable development and safety on earth depend on water (World Health Organization, 2010). It assists as a basis of water for native, agricultural and industrial usages and other growing initiatives (Ayazi et al., 2010; Nampak et al., 2014; Elbeih, 2015). Worldwide, groundwater delivers drinkable water to at least 50 percent of the global people & accounts for 43 percent water of the irrigation (Water, 2015). For a country like Egypt, groundwater is the second most significant source of freshwater. (Abd Ellah, 2020), and accounting for approximately 20 percent of Egypt's total water resource possibility (A. R. Allam et al., 2003). As a result, food security includes a high demand for potable water, as one of the Sustainable Development Goals (SDGs(, that is, to guarantee the availability and long-term management of water and sanitation (U.N, 2018). Under the influence of global change events, it is believed to be a major basis of forthcoming water supply, farming, irrigation and food fabrication (Clifton et al., 2010). Despite huge groundwater reserves, many countries face supply crisis and need to pay extra attention. Major aquifers of groundwater around the sphere are under burden to encounter the increasing water demands of growing inhabitants (Shahid & Hazarika, 2010) .Sustainable supervision of groundwater resources is a major challenge. One of the purposes of assessing groundwater resources is to deliver info on the existing state of reserve & gain insight into future groundwater availability (Reilly et al., 2008). Delineating the groundwater accessibility requires calculating the amount of groundwater in a region/aquifer. Groundwater is highly localized and spatially variable in the Aquifer. Groundwater movement and generation are determined by many factors, including topography, lithology, fissures, weathering, depth,

porosity, drainage, soils, climatic environments, and interrelationships among these elements. By properly estimating these parameters, we can fully understand the groundwater body (Selvam et al., 2014).

Geospatial methods are one of most popular approaches for rapidly delineating possible groundwater bodies in subsurface (Solomon & Quiel, 2006; Saha et al., 2010; Elewa & Qaddah, 2011). Geospatial methods are simpler, more consistent, and less expensive than traditional methodologies such as boreholes, hydrogeological, geological field studies, and geophysical approaches in assessing groundwater resources (Jha et al., 2010; Thapa et al., 2017a; Arulbalaji et al., 2019).

Various varieties of data & thematic maps can be used to identify potential groundwater areas, like satellite imagery, geological data, soil data , drainage data, & precipitation data (Machiwal et al., 2011; Srivastava et al., 2012; Lakshmi & Reddy,2018). Recently, numerous researchers have struggled to describe accessibility of groundwater using a variety of facts and knowledge data driven methods in combination with remote sensing (RS) & (GIS). Approaches based on data and knowledge reflect the diverse outlooks on spatial modeling (Rajabi et al., 2014; Andualem & Demeke, 2019).

A review of various literatures indicates that researchers have used a variety of methods to delineate potential groundwater bodies and map them. For example, some researchers apply probabilistic models such as: Multicriteria analysis (Akinlalu et al., 2017; Osinowo & Arowoogun, 2020), frequency ratio decision analysis (Elmahdy & Mohamed, 2015; Guru et al., 2017; Abu El-Magd & Eldosouky, 2021), weight of evidence (Pourtaghi & Pourghasemi, 2014), analytic hierarchy process (AHP) (Mukherjee & Singh, 2020), logistic regression (Nguyen et al., 2020), artificial neural network models & weight of evidence (Corsini et al., 2009), Shannon's Entropy (SE) & random forest (RF) (Zabihi et al., 2015), RF & Maximum Entropy

(Rahmati et al., 2016). Frequency ratio analysis (FR) for delineating groundwater probable zones by using well sites as an indicator applied by (Pourtaghi & Pourghasemi, 2014; Trabelsi et al., 2019). Trabelsi et al., (2019) used a probability basis frequency ratio model on the ground-water prospective of Medjerda area (Tunisia), and outcomes indicated a fairly satisfactory accurateness of 86%. Application of the Shannon entropy model in the ground water demarcation performed well, achieving higher accuracy than the FR model, demonstrating the quality and capability of this model in generating Groundwater potential maps GPMs (Naghibi et al., 2015; Hou et al., 2018).

Egypt is distinguished by its dry climate, low rainfall, desert terrain, and unreliable water resources (M. N. Allam & Allam, 2007). Egypt's water resource system is complicated and uncertain, so it is a great challenge and a need arises to address the rapidly wide gap for both limited water resources and increasing demand for freshwater. In modern times, Freshwater resources rank first among all natural resources on the earth. Fresh water is distributed in varying quantities everywhere (Abd Ellah, 2020).

Egypt in general suffers from the deficiency of freshwater, with less than thousand cubic meters of available freshwater per capita per year. Egypt's water consumption rate is about (190) L/person/day. In contrast, the exemplary (Middle Eastern and North African) diet requires (294) L of water per person per day (Elbeih, 2015). furthermore, the unmanaged resident’s development takes this issue to the worst. The same issue requires a complete investigation program to assign potential groundwater zones in the Suez governorate NE of Egypt moreover a managed strategy to monitor and control the random exploitation of recognized groundwater aquifers. For this purpose, we planned to integrate the two approaches (RF-PR and SE) to assess groundwater potential in areas where no groundwater studies

have been conducted so far according to the researchers' knowledge, with the exception of the study conducted by Abu El-Magd & Embaby, (2021), which dealt with the)north-western(region the (Gulf of Suez). A weighted GIS-based model with a linear equation approach was used in this study.

2. Geo - Characterization of Suez Governorate (SG)

Geographically, Suez Governorate (SG) is one of (six) governorates in Egypt located within the Suez Canal zone, It is also one of Egypt's (seven) economic zones established by the Egyptian government through the General Organization for Physical Planning (GOPP) (GOPP, 2014). It is currently witnessing several activities aimed at expanding agricultural, industrial, and tourism lands. The SG is located approximately 138.8 km east of Cairo, at the head of the Gulf of Suez between latitudes 28°57′ 36.46” and 30° 17’ 13.68″ North and longitudes 31° 50′ 39.32”and32° 51′ 12.82″ East, with a total shape area of approximately 9175.6 km2. It is bounded on the north by the governorates of (Ismailia) and (North Sinai), on the south by the governorates of (Beni Suweif) & the (Red Sea), eastward by the governorate of (South Sinai), and on the west by the governorates of (Cairo) and (Giza). The SG consists of (21) villages. Figure .1. As a result, the province of Suez stands out geographically, as it is located at the exit of the Suez Canal, one of the most important navigational outposts. The province's importance grew after the canal's construction, particularly with the establishment of seaports such as Suez, Ain Sukhna, and Adabiya, which aided the province's diversification of activities (GOPP, 2014).

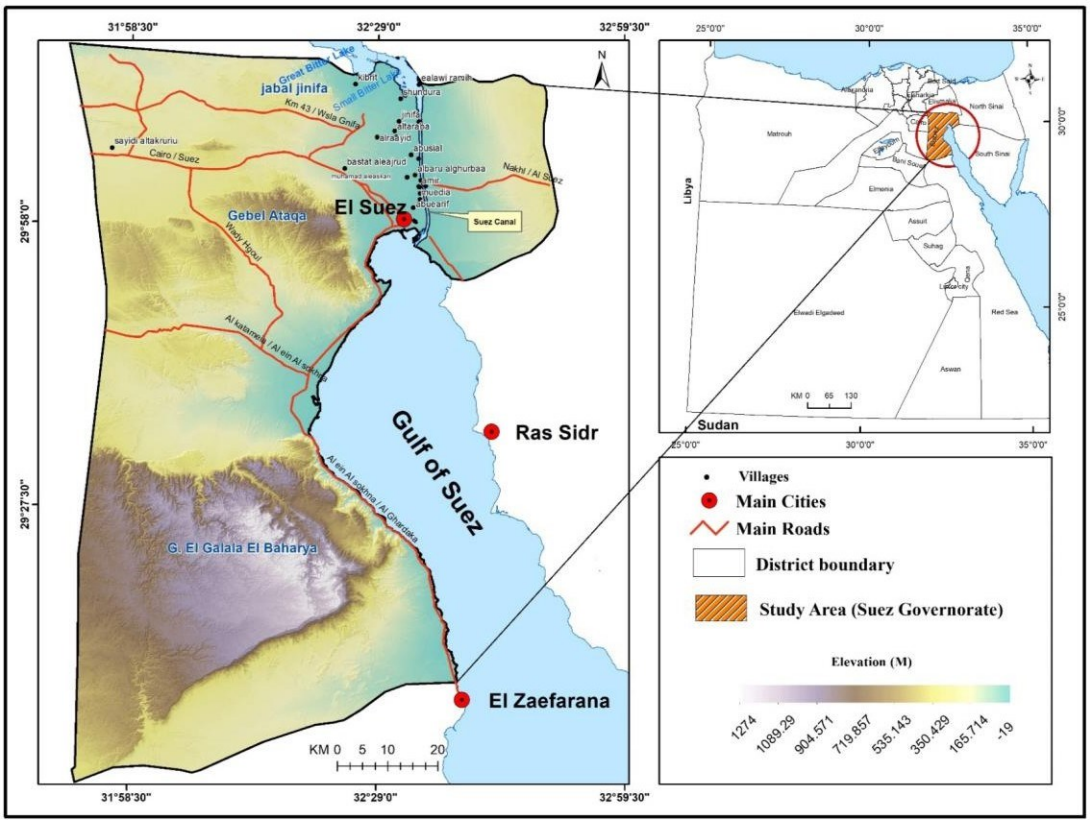

Figure. 1. geographic location of the SG. (Created by Egyptian General Survey Authority, scale 1 : 2000, 000, printed by the General Department of Topographic Maps in 2016, and it was reprinted in 2021/2020) .

The topography of the region is distinguished by a variety of hills, valleys, lakes, and a gentle sloping. It is surrounded on the north by the Gebel Ataqa and Jinifa, to the north-west by the Great and small bitter lakes, to the south by the (El Galala El Bahariya) plateau, and to the north-east by the (Gulf of Suez) Figure. 1. Many valleys descend from the Ataqa and Jinifa mountains and the (El Galala El Bahariya) plateau in the study area. These valleys involve Ghweiba, El Badaa, Okheider, Hommath, and Hagoul (Youssef et al., 2011). In general, the land surface in the SG inclines toward the Suez Canal,

peaking as it rises over 1200 metres above sea level in the governorate's west and falls to -19 metres below sea level in the Gulf of Suez. Figure .1.

various studies were conducted about the geological and hydrogeological conditions around SG (El Osta et al., 2010; El-Omla & Aboulela, 2012). Geologically, most of the unveiled rocks units overlay the SG are all sedimentary origin (El-Behiry et al., 2006). They extend in age from the Upper Carboniferous to Quaternary. (Upper, middle, lower Eocene deposits), Quaternary deposits and Miocene deposits are the more broadly rock units in this region. The Maadi Formation deposits of the upper Eocene appear in the central part of the Governorate; these deposits are composed of limestone and marl with some shale intrusions. Middle Eocene deposits, consisting of limestone, marl, and calcareous sandstone, appear in the centre and south of the SG. The Quaternary rocks are constituted by undifferentiated Quaternary sediments, which shrouded the valleys, alluvial fans and its coastal plain, including sand and gravel, the low area below the besetting mountains, thus, they access the coastline with sediments containing Sabkha sediments (consisting of silt, clay, evaporites), stabilized dunes and valleys sediments. The Miocene deposits that are exposed in the north and center of the SG, they composed of sand, gravel, limestone, marl, and some clay intrusions. Figure 8 (o) displays the details.

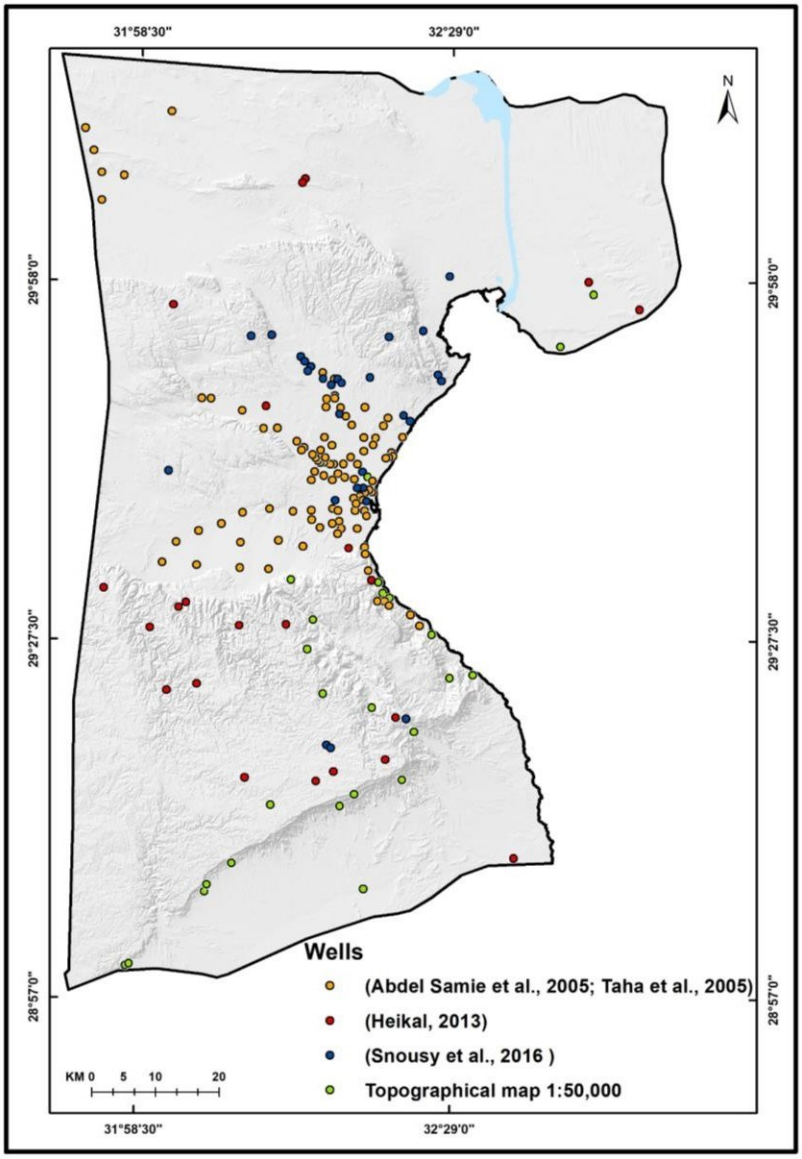

Figure. 2. samples wells of the SG

Hydrogeological, in SG, groundwater is mainly encountered in two several water-bearing aquifers (Salim, 2012): (a) the granular aquifers, The study area occupies parts of its coastal aquifer (It returns to the aquifer of the Quaternary), with a free water table ranging in depth from (9.4 meter) within east to (39.9 meter) within north-west

(El Osta et al., 2010), is composed of graded sand dispersed with lenses of clay and gravel deposits (Abu El-Magd & Embaby, 2021). (b)The (Nubian Sandstone aquifer), It is of Paleozoic Lower Cretaceous age and is made up of (shale & sandstone layers). The drilling depth varies between zero to 500 metres. The salinity range of water is from (1 to 4 thousand ppm). The Fissured Carbonate Aquifer, it returns to various geological ages and is composed of shale & sandstone classes, the drilling depth ranges between zero to 500 metres, and the water's salinity range is from (2,1 to 16 thousand ppm) (Hefny & Shata, 2004; Salim, 2012).

Climatology, SG is part of Egypt's arid ring, which is distinguished by long & hot summers, moderate temperature in the winter, rare rains, and high humidity rates because of the continuous sunshine and evaporation. Its climate is described as a desert climate. The climate here is classified as Bust/waist/hip measurements (BWh) by the Köppen-Geiger system (Zaghlol et al., 2016). depending on Suez Meteorological Station, During the period (1980 to 2017), In the area, the average yearly air temperature is around (22.4°C). Summers are dry and hot, with an average temp of)30.1°C(in August. The coldest months are December to February, where the average temp drops to)18.2 °C(and the coldest months is January reaching 10.5°C. Wind overwhelmingly blows from north, northwest directions. The rainfall here mean 16.3 mm. The highest average annual amount of rainfall was recorded in the autumn season 7.2 mm, The annual average of humidity is 57%, the average annual evaporation is 8.8 mm, the highest in August was 12.5 mm, and the lowest in January was 5.6 mm (Ahmed, 2018). Therefore, it is difficult to sustain rain-fed agriculture under these conditions (El-Kholei et al., 2004).

3. Materials and methods

Groundwater potential zones in the study site were assessed using GIS by creating and combine multiple thematic layers. Create

thematic layers for drainage density, lithology, topography, lineaments **&** slopes etc. Methodology section is classified into four steps: (1) 176 groundwater wells were preparing and were mapped in the SG (figure .2.). of the 176 wells sites, On the other hand, 27 wells were defined (topographical map at 1:50,000 scale of the military surveying authority, Egypt) and the remaining 149 well are collected from the previous studies distributed in the area (Abdel Samie et al., 2005; Taha et al., 2005; Heikal, 2013; Snousy et al., 2016). These wells were split into (2) groups at random: Training & Testing data. of the 176 wells, 132 (70%) were chosen for training, with the residual 44 (30 in percent) kept for verification. (2) Building a geospatial database as shown in Table 1 (3) The RF-PR and SE model are used to compute the weightage of groundwater potential factors. (4) results verification in a specific area is measured Groundwater prospects and accessibility by several interconnected factors, like lithology, structure in strata, landscape & climate. (Solomon & Quiel, 2006b; Chenini et al., 2010; Oh et al., 2011; Mogaji et al., 2016; Anbarasu et al., 2020).

In this study, we evaluate sixteen factors for this purpose. The software (ArcGIS 10,5) was used to create the geospatial data, and Microsoft Excel was used to calculate the weights for all factors and associated functions. To validate the results, a graph showing the output of each achieved groundwater potential category was used, a raster calculator tool in ArcGIS 10.5 software was used to produce the final map of GPZPm. the methods adopted in the current study are presented on the flowchart (Figure. 3.) and they are summarized in the following sections:

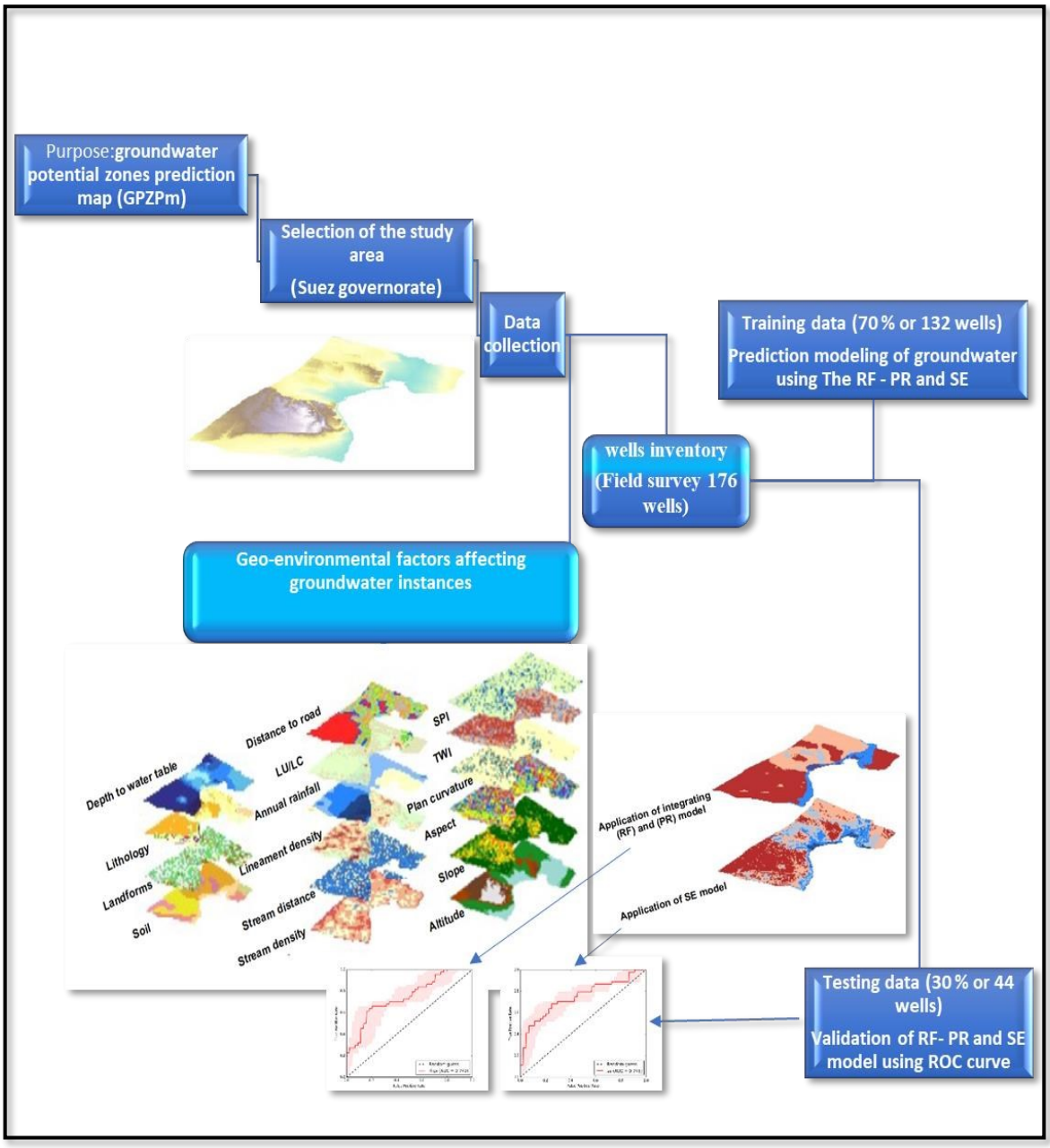

Figure. 3. the adopted methodology in the present study.

Table .1.

the factors used to determine groundwater potential mapping.

Factor	source of data & acquisition date	Resolution	data classification method
altitude slope aspect Plan curvature Topographic Wetness Index "TWI" Stream Power Index "SPI" stream density Distance to stream	https://spacedata.copernicus.eu - (01-2021)	Spatial resolution 30 m	*Manual* *natural break* *equal interval* *natural break* *Manual* *Manual* *natural break*
Lineament density & Lithology	Geology sheet survey (CONOCO Coral) – (1987)	Scale 1:500 000	*Manual* *natural break* *Lithological units*
Average annual Rainfall	(https://crudata.uea.ac.uk/cru/data/hrg) - (2011 - 2020)	30' x 30'	*Manual*
Landuse and Landcover (LU/LC)	Sentinel-2 L2A https://livingatlas.arcgis.com/landcover/ - (01- 01- 2021)	Spatial resolution 10 m	*artificial intelligence (AI)*
Distance to road	https://www.openstreetmap.org/relation/3062185#map=8/29.626/32.338 - (10 - 12 - 2021)	Scale 1:500 000	*Manual*
Soil	(http://www.un-spider.org/) & verified by (Hammad, 1975). (https://esdac.jrc.ec.europa.eu/images/Eudasm/Africa/images/maps/download/afr_egsma2.jpg) – (1975)	Scale 1:2,000, 000	*Soil unit*
landforms	https://spacedata.copernicus.eu – (01–2021)	Spatial resolution 30 m Topographic Position Index (Jenness) grid Jenness Enterprises - ArcView Extensions; Topographic Position Index	*Landform Classification (Jenness)*
Depth to water table (DTW)	- (Monsef & Smith, 2019) - (Salim, 2012) - (Snousy et al., 2016) (2008 – 2019)	Scale 1:500 000	*Manual*

4. Thematic maps

Altitude of surface acts as an important role in the recharge of groundwater (Thapa et al., 2018). It is the main cause of water movement caused by gravity (Gebreyohannes et al., 2017). As a result, the research area's elevation map was split into five categories. Figure 4 (a). For the groundwater slope gradient is also one of the important parameters in favor of water infiltration (Magesh et al., 2012). Areas with low slopes have low surface runoff & high infiltration rates (Bagyaraj et al., 2019). On the other hand, steep slopes favor rapid discharge of rainwater through runoff and drainage (Mogaji et al., 2015). The current research region was divided into five categories based on the degree of slope as shown in Figure 4 (b). The slope front facing side has a strong influence on hydrological parameters like evapotranspiration, precipitation direction, and weather process, particularly in dry and arid areas with little plant cover (Ercanoglu & Gokceoglu, 2002). Sides that rise from flat surfaces or gentle slopes allow settled water to pass fluidly, increasing infiltration capacity and resulting in more replenishment (Khan et al., 2020) . Nine classes of aspect were created in the aspect map ash shown in Figure 4 (c).

Plan curvature is described as the curvature of the contour line at the crossing of the horizontal surface and the ground, which influences potential for groundwater (Ding et al., 2017). and can be used to describe the divergence and convergence of flow and to distinguish between catchments and valleys guided by a zero-order hydraulic network (Catani et al., 2013). Likewise, surface curvature is significant because concave surfaces are best suited to holding surface water, which aids in recharging the zone. Plan curvature of our current research was categorized into three classes as shown in Figure 4 (d). Meles et al., (2020) explained that (TWI) is strongly related to soil wetness & groundwater levels and flow. The greater the (TWI) value,

the greater the prospect for groundwater (Mousavi et al., 2017; Kim et al., 2019). As shown, the (TWI) map was further classified into 4 classes in Figure 5 (e) was calculated based on the succeeding formula (Zhou et al., 2020): TWI = ln (AS / tan b), so AS = watershed area and (b) is the local slope.

SPI measures the destructive force of water currents in a catchment (W. Chen et al., 2018). As a result, it is regarded as a factor influencing groundwater modelling potential. In this research, SPI map Figure 5 (f) was calculated based on the succeeding formula: $SPI = AS * \tan b$, so AS = watershed area and (b) is the local slope. Streams or rivers are the major sources of recharging the aquifers. As a result, the area which lies nearby streams is more potential for the groundwater (Rahmati et al., 2016; Arabameri et al., 2020). The drainage system's properties govern the rate of groundwater recharge. As a result, assessing drainage properties is essential for assessing groundwater resources. In overall, the tighter the (drainage system), the lower the renewal rate of aquifer. Low (drainage density) promotes groundwater infiltration & accumulation (Singh et al., 2013).This map was classified into five classes as shown in Figure 5 (g). The drainage density is indicated by the narrow spacing of channels (Waikar & Nilawar, 2014). The patterns and densities of drainage provide vital info about groundwater resources (Rajaveni et al., 2014; Nasir et al., 2018). In similar researches, areas with drainage distances were favoured for groundwater recharge prospects (Moghaddam et al., 2015; Naghibi, Pourghasemi, & Dixon, 2015; Khan et al., 2020). In the current research the drainage distance is further classified into five classes. Area with less than 200 m class reflects more chances of groundwater as compared to other classes as shown in Figure 5 (h).

Lineaments originate from the tectonics events and define the surface geography and structural features of rocks/soil as well as raise

the secondary porosity where structural features are determined (Rajaveni et al., 2017). Lineament mapping is an essential element in hard rock regions where lineament features have a major influence on groundwater generation and movement (Singh et al., 2013). Moreover, numerous studies have revealed lineament density to be a significant determinant of groundwater recharge potential, like as (Selvam et al., 2016; Abijith et al., 2020). From Geology maps survey, linear features were determined, lineament density map was prepared and classified into six classes as shown in Figure 6 (i).

In continuity to hydrological causes, precipitation is also regarded as the main source of groundwater recharge (Shekhar & Pandey, 2015; Allafta & Opp, 2021). Dense rainfall intensity leads to rise groundwater recharge (Kotchoni et al., 2019). Per year annual rainfall map was produced and categorized into fiver more classes like shown in Figure 6 (j). Land use/land cover has a significant impact on groundwater availability, and recharge (Zomlot et al., 2017; Dibaba et al., 2020) Furthermore, (LULC) maps were derived from Esri Land Cover 2021 Sentinel-2 L2A imagery at (10m) resolution based on deep learning (AI) land classification model Produced by Impact Observatory (IO), Microsoft, and Esri (Karra et al., 2021). These land use/land cover were classified into six further classes as shown in Figure 6 (k). In our study, the distance to road were classified into six classes with 1000 m intervals as shown in Figure 6 (l). In addition, soils can also influence infiltration rates, influence groundwater recharge (Oh et al., 2011; Etikala et al., 2019). Figure 7 (m) depicts the soil map of the region, which was classified into seven types of classes. Geomorphological properties provide critical information about groundwater availability such as groundwater movement and occurrence (Machiwal et al., 2011; P. Mukherjee et al., 2012; Selvam et al., 2014; Barik et al., 2017; Das, 2019). In this study, the topographic position index (TPI) map is first prepared for landform classification using the Jennes algorithm, which is implemented as an

ArcGIS extension by Jenness, (2006). The minimum & maximum TPI values for a 1500m scale are -297.734 and 362.275, respectively. Following the creation of the TPI map, the landform classification map was created. As shown in figure 7 (n), the topographic surface was classified into ten landform types, were applied in this article (Weiss, 2001).

The physical appearance of the rocks/strata is referred to as lithology. Rock properties affect the movement of subsurface water. Geological/Petrological features set groundwater movement & porosity (Ayazi et al., 2010). The higher the lithic porosity, higher will be the groundwater storage capacity (Al Saud, 2010). Lithology is important in determining groundwater flux through channels, permeability, and occurrences (Zandi et al., 2016; Gnanachandrasamy et al., 2018). Lithology map in current research was categorized into twenty classes as shown in Figure 7 (o). Furthermore, depth to water table is an important parameter in groundwater studies (Agarwal & Garg, 2016; Arshad et al., 2020), In addition to aquifer geometry and properties, DWT can aid in determining groundwater flow direction, flow rate, and recharge (Shahinuzzaman et al., 2021). In our case DTW table map was classified into 5 classes with an interval of 10m as shown in Figure 7 (p).

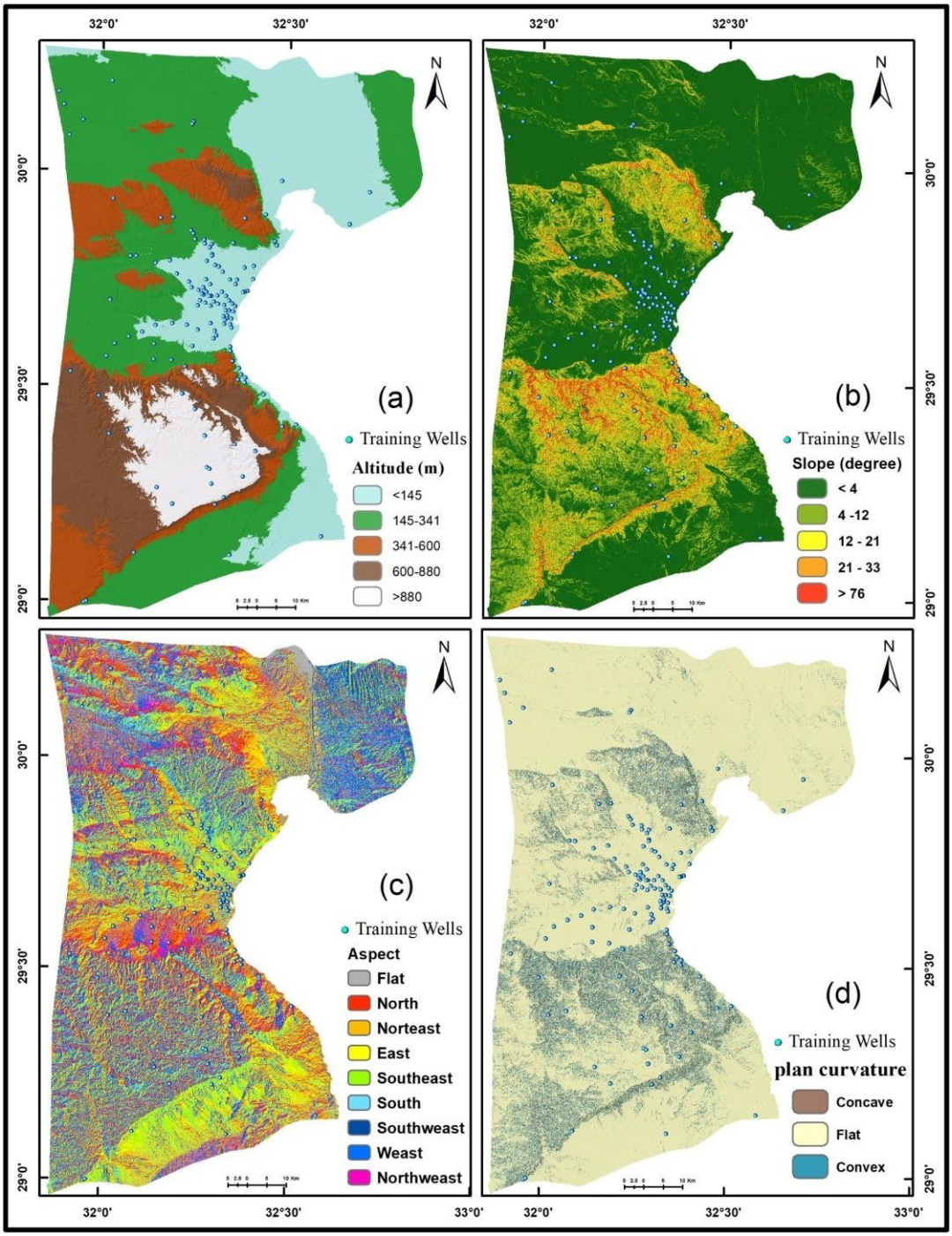

Figure 4: Altitude (a), Slope (b), Aspect (c), and plan curvature (d) map of study area.

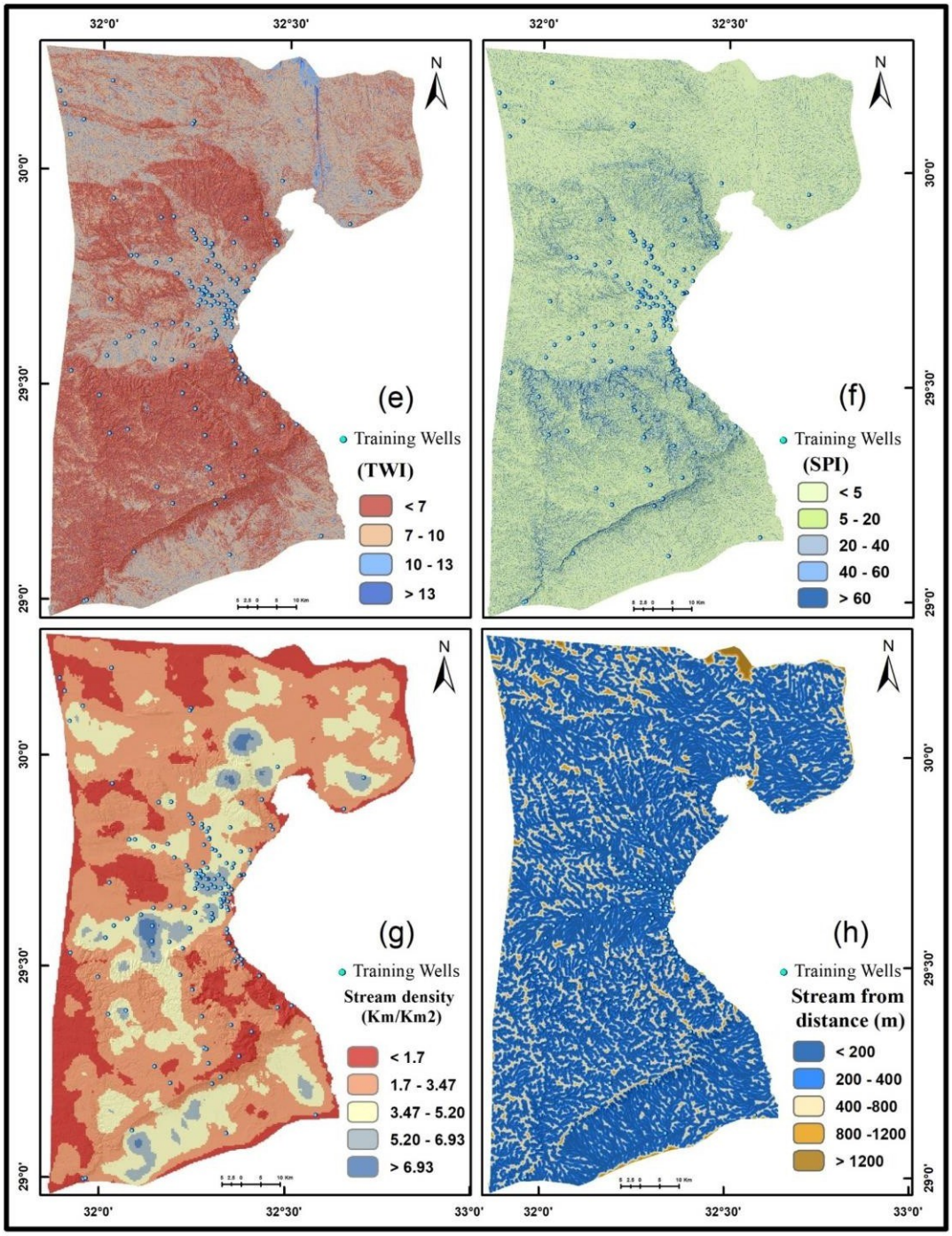

Figure 5: Topographic wetness index (e), SPI (f), Stream density (g), and Stream distance (h) maps.

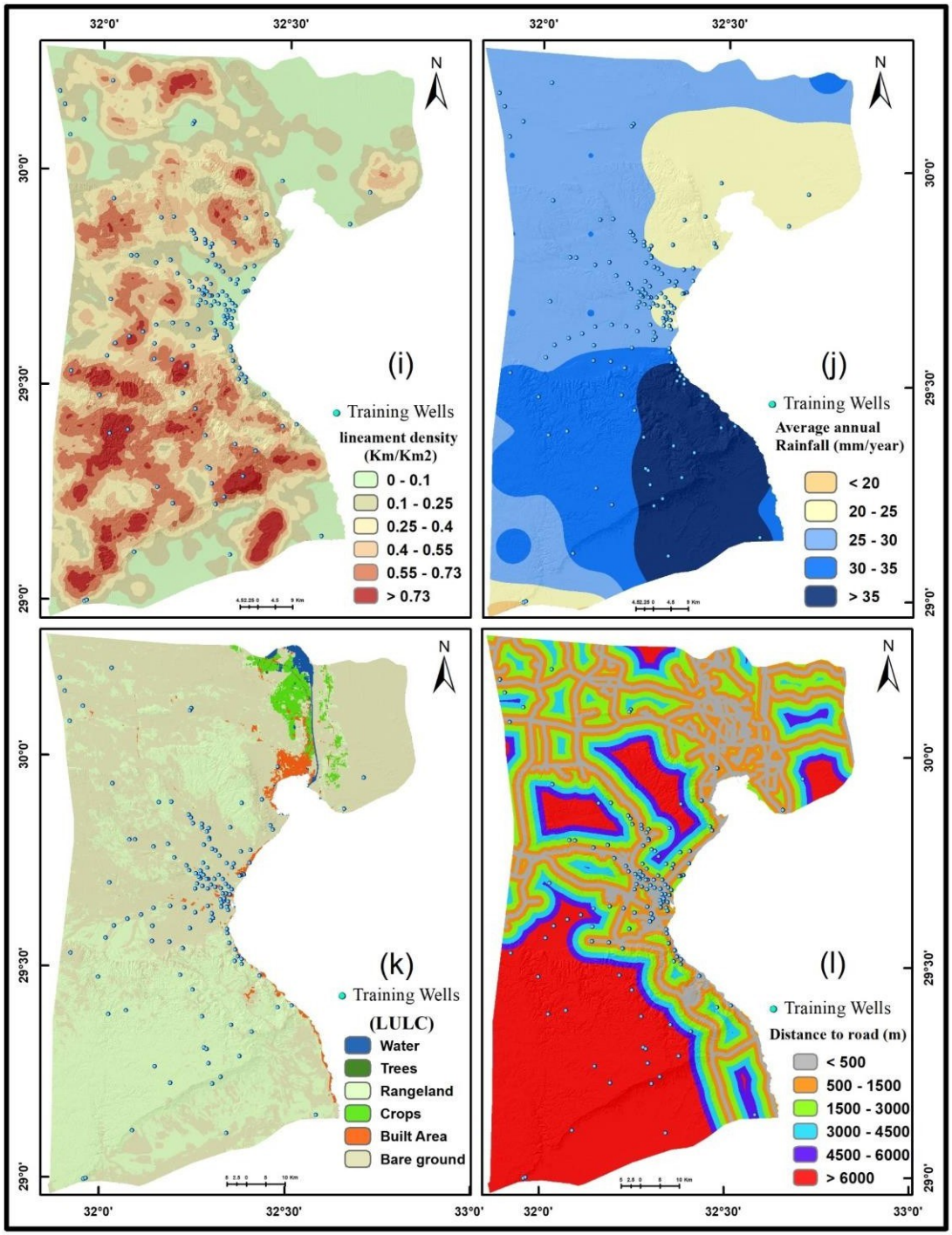

Figure 6: lineament density (i), Rainfall (j), Land use (k) and distance to road (l) maps.

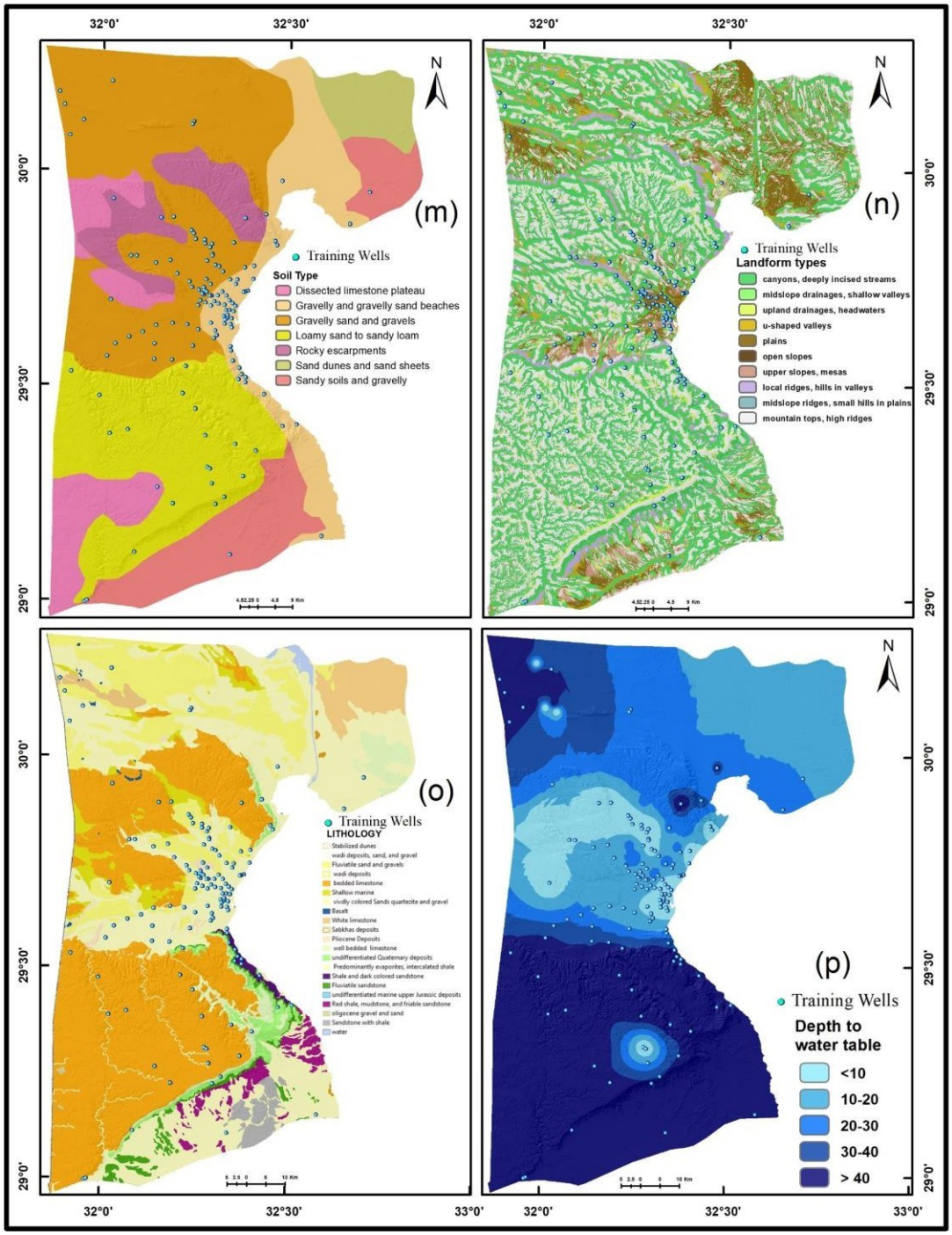

Figure 7: Soil (m), Landform types (n), lithology (o), and Depth to water table (p) maps.

Table 2

Weight of various Factors obtained from FR, RF-PR and SE

Factors	Classes	percent of (wells)	percent (Area)	*Fr*	*Rf* $=P_{ij}$	*pr*	SE			
							"P_{ij}"	"E_j"	"$1\text{-}E_j$"	"W_j"
Altitude (M)	<145	59.85	24.78	**2.415**	0.524	**4.827**	0.524	-0.147	0.191	**0.070**
	145-341	22.73	38.98	**0.583**	0.127		0.127	-0.114		
	341-600	5.30	13.99	**0.379**	0.082		0.082	-0.089		
	600-880	3.79	13.47	**0.281**	0.061		0.061	-0.074		
	>880	8.33	8.78	**0.950**	0.206		0.206	-0.141		
	-	**100**	**100**	**4.608**	-		**1.00**	**0.565**		
Slope (degree)	<4	78.03	62.80	**1.242**	0.242	**1.717**	0.302	-0.157	0.039	**0.014**
	4-12	7.58	19.03	**0.398**	0.078		0.097	-0.098		
	12-21	6.82	10.17	**0.670**	0.131		0.163	-0.128		
	21-33	6.06	6.15	**0.985**	0.192		0.239	-0.149		
	>76	1.52	1.84	**0.824**	0.161		0.200	-0.140		
	-	**100**	**100**	**4.120**	-		**1.00**	**0.672**		
Aspect	*flat*	8.33	7.21	**1.155**	0.130	**1.012**	0.130	-0.115	0.022	**0.008**
	n	10.61	12.80	**0.829**	0.094		0.094	-0.096		
	ne	13.64	12.20	**1.118**	0.126		0.126	-0.113		
	e	15.15	12.51	**1.211**	0.137		0.137	-0.118		
	se	15.91	11.98	**1.328**	0.150		0.150	-0.124		
	s	17.42	12.83	**1.358**	0.153		0.153	-0.125		
	sw	8.33	11.69	**0.713**	0.080		0.080	-0.088		
	w	5.30	10.65	**0.498**	0.056		0.056	-0.070		
	nw	5.30	8.14	**0.652**	0.074		0.074	-0.083		
	-	**100**	**100**	**8.862**	-		**1.00**	**0.933**		
Plan curvature	Concave	5.30	5.93	**0.894**	0.342	**1.385**	0.342	-0.159	0.012	**0.005**
	Flat	89.39	86.35	**1.035**	0.396		0.396	-0.159		
	Convex	5.30	7.71	**0.687**	0.263		0.263	-0.153		
	-	**100**	**100**	**2.617**	-		**1.00**	**0.471**		

Table 2. *Cont*.

Factors	Classes	percent of (wells)	percent (Area)	*Fr*	*Rf* $=P_{ij}$	*pr*	SE			
							"P_{ij}"	"E_j"	"$1-E_j$"	"W_j"
TWI (100/m)	<7	24.24	41.43	**0.585**	0.123		0.123	-0.112		
	7-10	52.27	42.44	**1.232**	0.259		0.259	-0.152		
	10-13	16.67	11.58	**1.439**	0.303	**1.999**	0.303	-0.157	0.038	**0.014**
	>13	6.82	4.56	**1.497**	0.315		0.315	-0.158		
	-	**100**	**100**	**4.753**	-		**1.00**	**0.579**		
SPI (100/m)	<5	70.45	64.09	**1.099**	0.233		0.233	-0.147		
	5-20	10.61	15.97	**0.664**	0.141		0.141	-0.120		
	20-40	5.30	5.98	**0.886**	0.188		0.188	-0.137		
	40-60	3.03	2.72	**1.116**	0.237	**1.000**	0.237	-0.148	0.010	**0.004**
	>60	10.61	11.24	**0.944**	0.200		0.200	-0.140		
	-	**100**	**100**	**4.709**	-		**1.00**	**0.692**		
Stream density (KM/KM2)	<1.7	11.36	20.16	**0.564**	0.061		0.061	-0.074		
	1.7 - 3.47	39.39	52.55	**0.750**	0.081		0.081	-0.089		
	3.47 - 5.20	32.58	22.76	**1.431**	0.156		0.156	-0.126		
	5.20 - 6.93	15.15	3.95	**3.835**	0.417	**70.939**	0.417	-0.158	0.138	**0.051**
	> 6.93	1.52	0.58	**2.621**	0.285		0.285	-0.155		
	-	**100**	**100**	**9.201**	-		**1.00**	**0.602**		
Stream from distance (m)	<200	62.12	47.72	**1.302**	0.473		0.473	-0.154		
	200 - 400	25.76	30.28	**0.851**	0.309		0.309	-0.158		
	400 -800	12.12	20.22	**0.599**	0.218	**22.636**	0.218	-0.144	0.348	**0.128**
	800 -1200	0.00	1.46	**0.000**	0.000		0.000	0.000		
	> 1200	0.00	0.32	**0.000**	0.000		0.000	0.000		
	-	**100**	**100**	**2.752**	-		**1.00**	**0.456**		

Table 2. *Cont.*

Factors	Classes	percent of (wells)	percent (area)	*Fr*	$Rf = P_{ij}$	*pr*	SE			
							"P_{ij}"	"E_j"	"$1-E_j$"	"W_j"
Lineament density (KM/KM_2)	0 - 0.1	31.82	20.31	**1.567**	0.274		0.274	-0.154		
	0.1 - 0.25	20.45	19.56	**1.046**	0.183		0.183	-0.135		
	0.25 - 0.4	25.76	19.87	**1.296**	0.226		0.226	-0.146		
	0.4 - 0.55	9.85	20.10	**0.490**	0.086		0.086	-0.091	0.047	**0.017**
	0.55 - 0.73	8.33	15.35	**0.543**	0.095	**33.340**	0.095	-0.097		
	> 0.73	3.79	4.81	**0.787**	0.137		0.137	-0.118		
	-	**100**	**100**	**5.729**	-		**1.00**	**0.742**		
Average annual Rainfall (mm / year)	<20	0.00	0.26	**0.000**	0.000		0.000	0.000		
	20 -25	25.76	19.53	**1.319**	0.337		0.337	-0.159		
	25-30	47.73	44.41	**1.075**	0.274		0.274	-0.154		
	30-35	12.12	20.26	**0.598**	0.153	**22.973**	0.153	-0.125	0.162	**0.059**
	> 35	14.39	15.54	**0.926**	0.236		0.236	-0.148		
	-	**100**	**100**	**3.918**	-		**1.00**	**0.586**		
LU/LC	Water	0.00	0.60	**0.000**	0.000		0.000	0.000		
	Trees	0.00	0.03	**0.000**	0.000		0.000	0.000		
	Crops	0.00	1.77	**0.000**	0.000		0.000	0.000		
	Built Area	6.82	1.41	**4.829**	0.722	**85.291**	0.722	-0.102	0.573	**0.210**
	Bare ground	68.18	53.83	**1.267**	0.189		0.189	-0.137		
	Rangeland	25.00	42.36	**0.590**	0.088		0.088	-0.093		
	-	**100**	**100**	**6.686**	-		**1.00**	**0.332**		
Distance to road (m)	<500	26.52	14.44	**1.836**	0.292		0.292	-0.156		
	500 - 1500	25.76	18.00	**1.431**	0.228		0.228	-0.146		
	1500 - 3000	18.94	16.24	**1.166**	0.185		0.185	-0.136		
	3000 - 4500	6.82	9.44	**0.722**	0.115	**37.688**	0.115	-0.108	0.057	**0.021**
	4500 - 6000	3.79	6.06	**0.625**	0.099		0.099	-0.100		
	> 6000	18.18	35.81	**0.508**	0.081		0.081	-0.088		
	-	**100**	**100**	**6.288**	-		**1.00**	**0.734**		

Table 2. *Cont*.

Factors	Classes	percent of (wells)	percent (Area)	*Fr*	$Rf=P_{ij}$	*pr*	SE			
							"P_{ij}"	"E_j"	"$1-E_j$"	"W_j"
Soil units	Dissected limestone plateau	0.76	8.77	**0.086**	0.015	**386.388**	0.015	-0.027	0.347	**0.128**
	Gravelly sand & gravels	40.91	32.74	**1.250**	0.215		0.215	-0.144		
	Loamy sand to sandy loam	14.39	22.73	**0.633**	0.109		0.109	-0.105		
	Sand dunes and sand sheets	0.00	4.33	**0.000**	0.000		0.000	0.000		
	Sandy soils and gravelly	2.27	12.66	**0.179**	0.031		0.031	-0.047		
	Gravelly and gravelly sand beaches	38.64	12.07	**3.200**	0.552		0.552	-0.143		
	Rocky escarpments	3.03	6.69	**0.453**	0.078		0.078	-0.086		
	-	**100**	**100**	**5.802**	-		**1.00**	**0.551**		
Landform types	Canyons and deeply	36.36	38.07	**0.955**	0.081	**35.068**	0.081	-0.088	0.072	**0.027**
	mid-slope drainages and shallow valleys	3.79	2.70	**1.400**	0.119		0.119	-0.110		
	headwaters and upland drainages	1.52	2.14	**0.709**	0.060		0.060	-0.073		
	valleys shaped like an u	6.82	4.55	**1.499**	0.127		0.127	-0.114		
	Plains	14.39	8.70	**1.654**	0.140		0.140	-0.120		
	slopes that are open	0.00	0.27	**0.000**	0.000		0.000	0.000		
	upper slopes and mesas	6.06	3.77	**1.609**	0.136		0.136	-0.118		
	local ridges and valley hills	6.82	3.33	**2.049**	0.174		0.174	-0.132		
	Plains with small hills and midslope ridges	3.79	2.88	**1.315**	0.111		0.111	-0.106		
	mountain peaks and high ridges	20.45	33.59	**0.609**	0.052		0.052	-0.066		
	-	**100**	**100**	**11.799**	-		**1.00**	**0.928**		

Table 2. *Cont.*

Factors	Classes	percent of (wells)	percent (Area)	*Fr*	*Rf* $=P_{ij}$	*pr*	SE			
							"P_{ij}"	"E_j"	"$1-E_j$"	"W_j"
Lithology	Stabilized dunes	0.00	3.44	**0.000**	0.000	**4.033**	0.000	0.000	0.387	**0.142**
	wadi deposits, sand, & gravel	12.88	12.23	**1.053**	0.035		0.035	-0.051		
	Fluviatile sand and gravels	9.85	12.83	**0.767**	0.025		0.025	-0.040		
	wadi deposits	40.91	15.67	**2.610**	0.086		0.086	-0.092		
	bedded limestone with local chert	15.91	36.68	**0.434**	0.014		0.014	-0.026		
	Shallow marine shale &limestone	0.76	3.03	**0.250**	0.008		0.008	-0.017		
	vivdly colored Sands quartezite & gravel	2.27	3.94	**0.577**	0.019		0.019	-0.033		
	Basalt	0.00	0.11	**0.000**	0.000		0.000	0.000		
	White limestone	0.00	0.74	**0.000**	0.000		0.000	0.000		
	Sabkhas deposits	0.00	0.08	**0.000**	0.000		0.000	0.000		
	Pliocene Deposits	3.03	0.57	**5.303**	0.174		0.174	-0.132		
	limestone with minor water carbonate	4.55	3.04	**1.497**	0.049		0.049	-0.064		
	undifferentiated Quaternary deposits	4.55	2.06	**2.208**	0.073		0.073	-0.083		
	Predominantly evaporites, intercalated shale	3.79	0.32	**12.018**	0.395		0.395	-0.159		
	Shale and dark colored sandstone	1.52	0.40	**3.835**	0.126		0.126	-0.113		
	Fluviatile sandstone with wadi deposits	0.00	1.35	**0.000**	0.000		0.000	0.000		
	Jurassic deposits	0.00	0.01	**0.000**	0.000		0.000	0.000		
	Red shale, mudstone & friable sandstone	0.00	1.64	**0.000**	0.000		0.000	0.000		
	oligocene gravel & sand	0.00	0.04	**0.000**	0.000		0.000	0.000		
	Sandstone with shale	0.00	1.39	**0.000**	0.000		0.000	0.000		
	water	0.00	0.45	**0.000**	0.000		0.000	0.000		
	-	**100**	**100**	**30.552**	-		**1.00**	**0.811**		
Depth to water table (m)	<10	34.09	7.43	**4.587**	0.621	**106.27**	0.621	-0.129	0.280	**0.103**
	10-20	25.76	21.39	**1.204**	0.163		0.163	-0.128		
	20-30	8.33	18.52	**0.450**	0.061		0.061	-0.074		
	30-40	5.30	10.05	**0.528**	0.071		0.071	-0.082		
	> 40	26.52	42.61	**0.622**	0.084		0.084	-0.090		
	-	**100**	**100**	**7.391**	-		**1.00**	**0.503**		

5. Modeling Techniques

5.1 Frequency ratio

FR is a popular statistical method applied in geospatial assessment of probabilistic relationships among various variables (Razandi et al., 2015; Ahmadi et al., 2021). A number of researches have demonstrated the use of frequency ratios to determine local groundwater potential (Pourtaghi & Pourghasemi, 2014; Falah & Zeinivand, 2019; Das, 2019; Ahmadi et al., 2021). Based on the observed relationships and correlations between various conditioning factors, this model was built (Table 2). and can be expressed mathematically by (Pham et al., 2015; Acharya & Lee, 2019).

$$FR = \frac{N_{pi}\,(LX_i)/\sum_{i=1}^{m} N_{pi}\,(LX_i)}{N_{pi}\,(X_j)/\sum_{j=1}^{n} N_{pix}\,(Lj)} \qquad \text{(i)}$$

In equation 1, FR= frequency ratio of category *(i)* of *(j)* parameter. Npix (LXi) is equal to Number of wells pixels with category *(i)* of variable *(X)*. whereas the Npix *(Xj)* are the pixels Number with variable Xi, and number of parameter represented by n.

In the succeeding step, FR were standardized in range of possibility values like 0,1 as RF (relative frequency) and was calculated by equation (ii)

$$RF = \frac{FR_{ij}}{\sum_{i=1}^{m} FR_{ij}} \qquad \text{(ii)}$$

After the standardization there was still drawback in equal weight of all factors, to slove this drawback prediction rate was calculated by using equation (iii),

$$PR = \left(\frac{RF_{max} - RF_{min}}{RF_{max} - RF_{\min}}\right) \quad \text{(iii)}$$

Finally, the GPZPm (groundwater potential zones prediction maps) were calculated by equation (iv),

$$GPZPm = \sum(PR * RF) \quad \text{(iv)}$$

5.2 Shannon Entropy

Generally, entropy indicates the degree of anomaly among events and outcomes or judgments on the numerous topics discussed (Wan, 2009; Amiri et al., 2014), where the entropy index is ratio of unit groups to system varied ratios and is defined as mean difference of uncertainties (Ihara, 1993; L. Chen et al., 2021). SE modified according to the Boltzmann technique was used as information system (Pourghasemi et al., 2012). SE model was applied on flood susceptibility (Yariyan et al., 2020) and for landslide vulnerability (Perera et al., 2019), leading to practical results. The resulting formula represents the embedded information of weight calculation. Vj is factor rank from the entire number (Bednarik et al., 2010) and is represented by

$$Eij = FR / \sum_{j=1}^{M} FR \qquad \text{(iii)}$$

In equation FR denotes the frequency ratio & Eij signifies probability density.

$$Hj = -\sum_{i=1}^{Mj} Eij \log_2 Eij,\ \mathrm{j} = 1, \ldots, \mathrm{n}, \qquad \text{(iv)}$$

$$H_{jmax} = \log_2 M_j, M_{j-number\ of\ classes} \qquad \text{(v)}$$

$$I_J = (H_{jmax} - \frac{H_j}{H_{jmax}}) \qquad \text{(vi)}$$

$$I = (0, 1), j = 1, .., \qquad \text{(vii)}$$

$$Vj = IjFR, \qquad \text{(viii)}$$

Finally, the GPZPm (groundwater potential zones prediction maps) were calculated by equation (ix),

$$GPZPm = \sum_{i=1}^{n} z/mi \times C \times W_j \qquad \text{(ix)}$$

In the above equations, *(Hj)* & *(Hjmax)* are the values of entropy, and *(Ij)* is the data factor, M is the amount of classes. Furthermore, Vj characterizes the entire weight value achieved for factor which ranges from (0:1), with values near one indicating more

confusion and variation (Al-Abadi et al., 2016; Khosravi et al., 2018). *(i)* is amount of specific parameter map, and *(z)* is the amount of classes within the parameter map through highest amount of classes, along with *(mi)* is amount of classes in specific parameter map, whereas *(C)* is the assessment of category afterward secondary sorting, & *(Wj)* represents factor weights (Bednarik et al. 2010)

6. Results and Discussion

6.1 FR Interpretation

In Frequency ratio interpretation higher FR reveals the important spatial association of training factors with the GW occurrences (Al-Abadi et al., 2016; Das, 2019), the standards greater than 1 display a resilient association and those lesser than 1 signify a weak association. The FR, RF and PR were used in current study to classify the association between each causal factors and GW occurrences as the outcomes are discussed in table 2.

The obtained results reflects that the lesser the altitude, the greater the influence on groundwater resources. So, the classes below 145 m with RF of 0.524 each have the most influence on groundwater resources. Moreover, slopes of < 4 with RF of 0.242 respectively have the most influence on groundwater resources. As for curvature, the flat curvature (0.396) has a strong influence on the GW resources in target area, which corresponds the nature of the groundwater resources.

Therefore, runoff penetrates more in flat areas than in other areas. On slopes, the east receives less sunlight than other slopes, which has a greater impact on groundwater resources (0.137). Followed by southeast (0.150) and south (0.153). As a consequence of investigating the association between precipitation and groundwater using Relative Frequency, it was found that precipitation of 20-25 mm has a great influence on groundwater (0.337). For soil type, the RF

results with a value of (0.215) indicate that gravel sand and gravel in rocky outcroppings with dunes have a significant impact on groundwater resources. It is worth noting that much of this zone is enclosed by the abovementioned soils.

For the land use, results reveal that built-up areas have a significant impact on groundwater resources (0.722). As for geology conditioning factors, mainly evaporated and intercalated shale (0.395) has a major impact on groundwater as compared to shale and dark sandstone (0.126). But some regions don't have enough RF. Regarding distance to the road, the RF results display that only classes above 6000 m have no impact on groundwater resources, while distances below 500 m have a significant influence on groundwater. First class i.e < 500 m (0.292), impact on groundwater resources is greatest, the farther the road, the smaller the effect on groundwater resources. The distance to road results display that the first class, < 500 m, has the greatest impact on groundwater and followed by class 500-1500 m (0.228). Lineament density results show that the first class, 1 km/km2, has the greatest impact on groundwater, followed by classes 0.25-0.4 km/km2 (0.226).A TWI grade of >13 has a large impact on groundwater at RF (0.315) and a grade of <7 has a low impact of 0.123 over GW. SPI classes between 40 and 60 have a large impact on GW with RF values (0.237). Steam density classes 5.20 to 6.93 can affect the GW with RF (0.417) value. The stream distance less than 200m have the greatest impact on groundwater distribution with RF (0.473), while other classes are negligible. Topography also plays an important role in groundwater distribution, as flat terrain has the largest impact on RF (0.140) in this study compared to other landscape features. Groundwater depth can affect groundwater, in which case class <10 has the highest RF (0.621).

The concluding groundwater yield index of target area was acquired using equation (ii) and is shown on the map in Figure 8 (a). Using the natural break classification in GIS, the resulting GPZPm

were categorized as low, very low, moderate, high, & very high. As table 3 summarizes the areas occupied through each of these factor's classes of RF-PR and Shannon entropy. Here, high-very high class covers area of 12% (1093 km2). Low, very low to moderate gradients occur within 88% (8013 km2) of target area, representing small efficiency of the aquifer system.

6.2 SE model interpretation

For current target area, SE model was also implemented to delineate the association among each training factor and GW distribution (Table 2&3). Weights evaluated of all the factors through SE which include Land use (0.210), geology (0.142), depth of water table (0.103), soil unit and stream distance (0.128) shows a highest impact as compared to all other factors evaluated. The assessed weights of SE for other training factors are as follows; Plan curvature (0.005), aspect (0.008), slope angle (0.014), altitude (0.070), TWI (0.014), SPI (0.004), stream density (0.051), lineament density (0.017), rainfall (0.059), distance to road (0.021), landform (0.027). The evaluated result shows that land use and geology have the highest impact, and the next are depth of water table, soil and stream distance. Normally, the most and the least vital factors for GW potentials in research area are lineament density, stream density, plan curvature and SPI, respectively.

The outputs acquired from the SE model in target region Table .2., have shown that (altitude, geology, soil, & slope) were regarded as the more vital parameters prompting GW efficiency conditions. The final groundwater potential index map was established by using equation ix. The acquired GPZPm was also categorized into 5 classes, basis on natural break classification, Figure 8 (b). Final map reflects that high - very high classes spread over a zone of 13 % (1193 km2) and moderate, low to very low cover an area of 87 % (7915.12km2)

round about reliable with the outcomes of RF-PR model (Table 3) & (Figure 8 and 9 a.b).

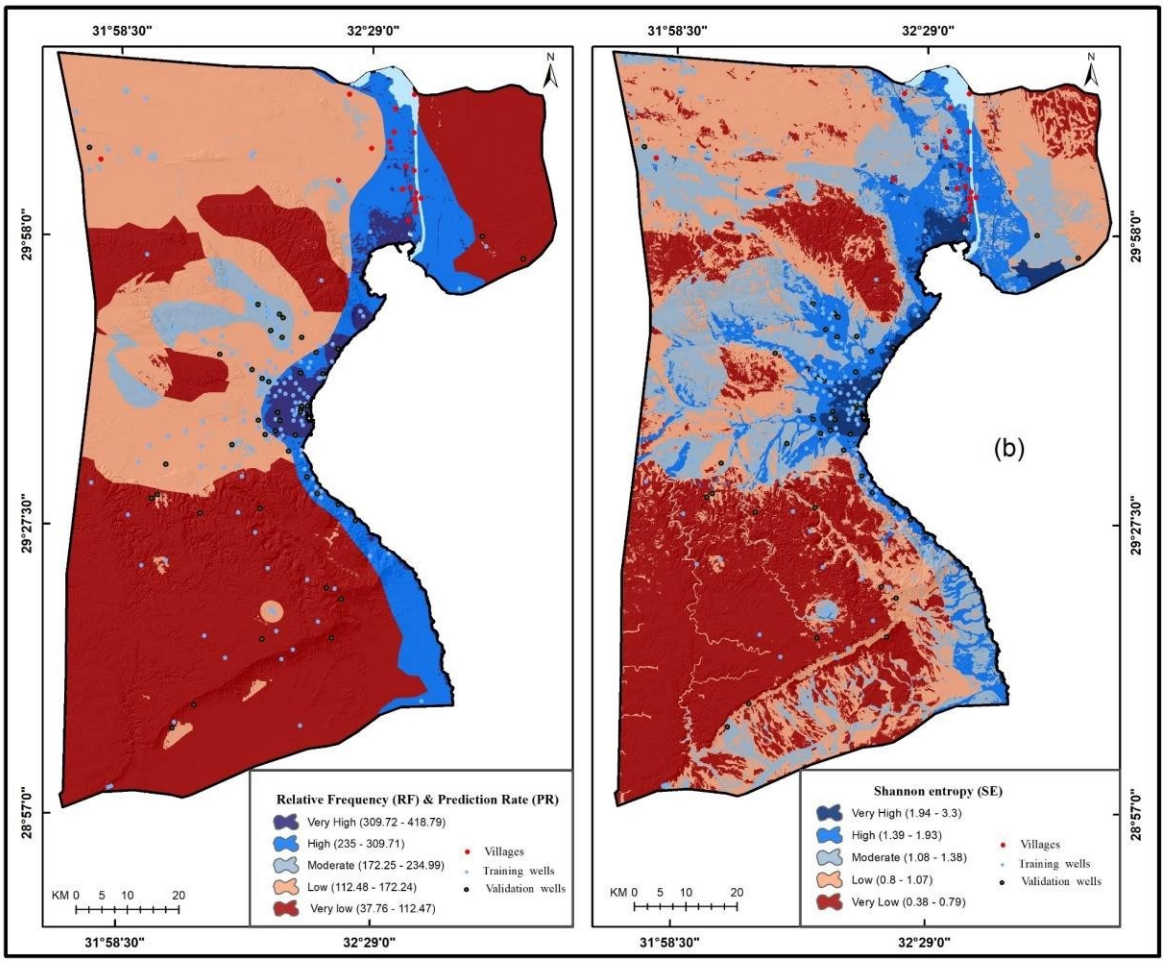

Figure 8: Final maps RF-PR (a) & SE (b) of GPZPm in study area.

Table 3

Coverage zones of various groundwater potential regions

GPZPm category	Relative Frequency (RF) and Prediction Rate (PR)			Shannon entropy (SE)		
	Range	Area *(present)*	Area *(km²)*	Range	Area *(present)*	Area *(km²)*
Very high	309.72 – 418.79	**2.64**	**240.36**	1.94 – 3.3	**2.60**	**236.92**
High	235 – 309.71	**9.38**	**853.93**	1.39 – 1.93	**10.50**	**956.16**
Moderate	172.25 – 234.99	3.84	350.12	1.08 – 1.38	21.48	1956.61
Low	112.48 – 172.24	32.54	2964.3	0.8 – 1.07	31.83	2899.15
Very low	37.76 – 112.47	51.60	4699.69	0.38 – 0.79	33.59	3059.36

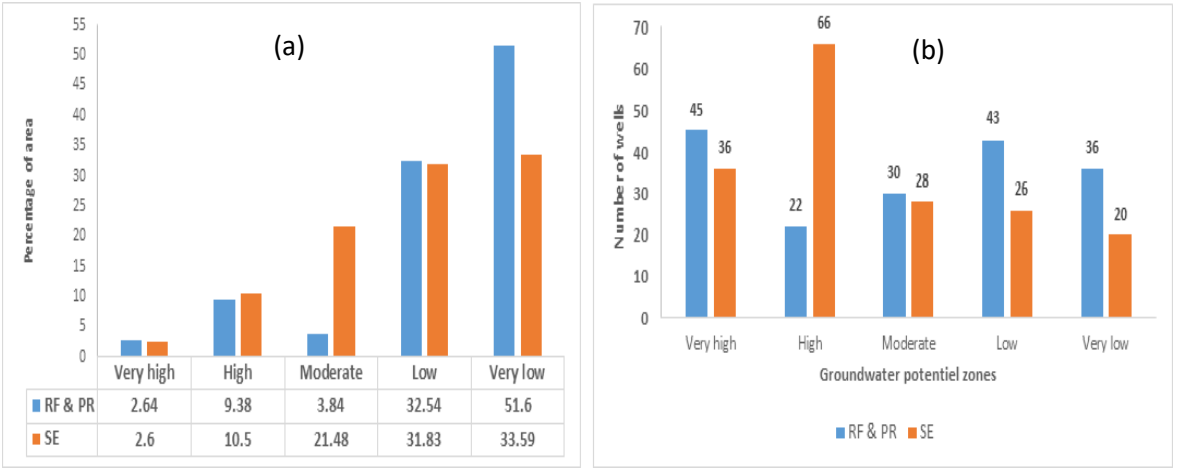

Figure 9: Ratio of RF-PR and SE (a) with area coverage and total number of existing wells (b) in each potential zone.

7. Results Validation

Predictive models (deterministic or probabilistic) require authentication earlier so that they can be used for forecasting requirements. Without validation, a model has no technical meaning (Chung & Fabbri, 2003). With reference to this, Curves of receiver operating characteristic (ROC) are commonly applied to study the value of both deterministic, probabilistic finding and prediction systems (Swets, 1988). ROC curve plots the model's sensitivity (the model correctly predicted the percentage of well pixels) and 1 specificity (proportion of well pixels predicted versus total). AUC designates the value of a predictive structure in terms of system capacity to properly predict the incidence or nonoccurrence of predetermined actions (Devkota et al., 2013). The model's predictive ratio is good when AUC equal 1 to 9. Like very good ranges 0.8-0.9, next good 0.8 up to 0.7, with average 0.7-0.6, and bad ranges from 0.6 to 0.5 (Yesilnacar & Topal, 2005). In the current research, AUC was obtained using the (roc) curve for both training (rate of success) **&** testing (prediction rate) for both models in a completely automated process using the (ArcSDM) extension, which was incorporated into ArcGIS Software (Wang et al., 2020). AUCs for both RF-PR and Shannon models are 0.749 and 0.745 (Figure. 10 a,b), correspondingly, indicating that RF-PR outperforms the Shannon's model.

In addition, the GPZPm results were matched to the distribution of groundwater wells, rural communities, and agricultural, reclaimed lands east and west of the Suez Canal (north of the study area), which mirrored the GW overview. The GPZPm is compatible with these groundwater sustainability indicators (Figure. 11). Fieldwork and high spatial resolution satellite imagery were used to collect these indicators.

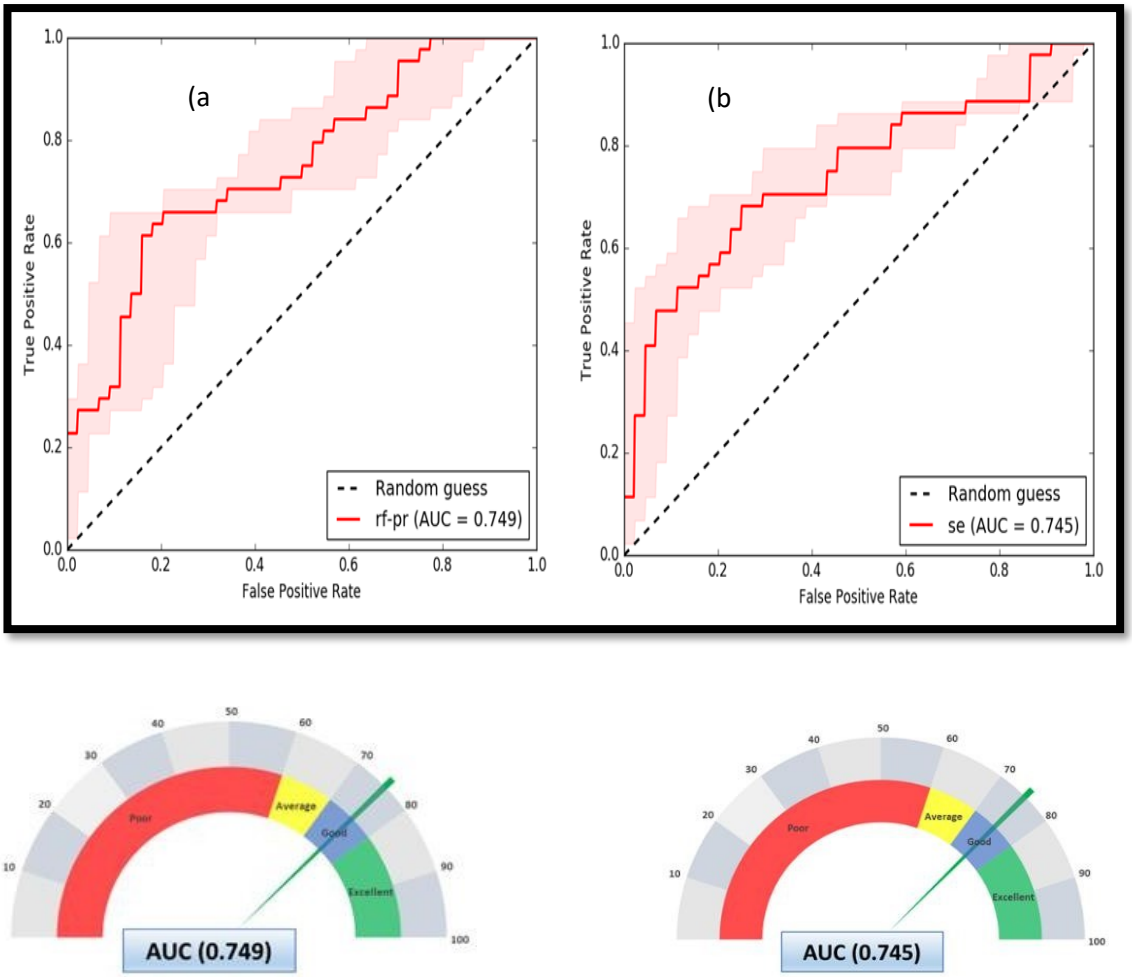

Figure 10: AUC for the RF-PR model (a) and SE model (b) with Gauge Chart.

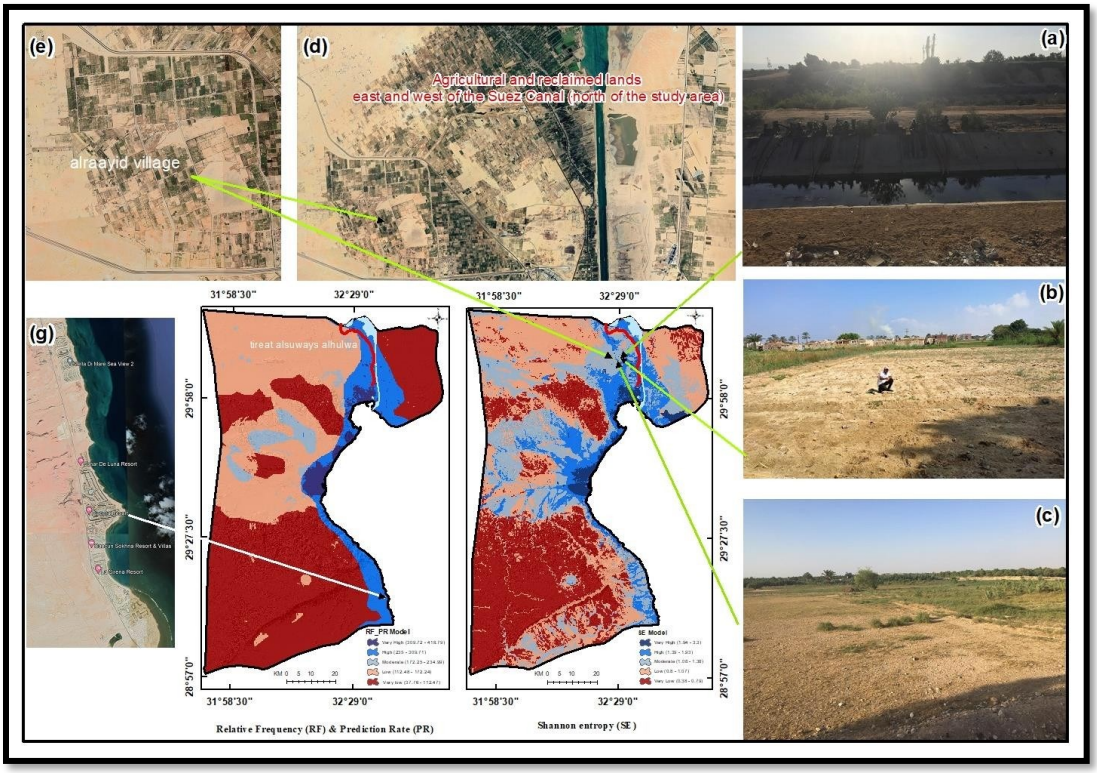

Figure 11: The groundwater potential zones prediction map in area.)a-b-c images) obtained during field surveys, shows the suffering of reclaimed lands to access water and Google Earth images (d-e-g) were used to verify the good and very good potential zones for GW. The images display the distribution of the GW wells, rural communities, tourism and agricultural areas.

8. Conclusions

GW resources play a progressively important part in supply of water worldwide, whereas assessing these zones of groundwater potential is a hot topic for government officials, groundwater agencies, private planners, and land use developers. In current research, two data driven models, i.e., RF-PR, and SE were effectively applied to demarcate the GW potential of the Suez governorate. Sixteen groundwater controlling factors from spatial

databank (Lithology, landform, soil condition, lineament distance, drainage density & distance, slope, distribution of rainfall, plan curvature, aspect, DTW, distance to roads, elevation, land use/cover, SPI & TWI) were chosen and evaluated in the ArcGIS software & groundwater potential zones prediction maps (GPZPm) were acquired. Soil, depth to water table and land use/cover were ranked highest in RF-PR, and land use, lithology, and depth to water table were ranked high in SE model. Lastly, by using the afore-mentioned two models, two GW potential maps were created. Following by AUC curve presented that the two models show reflects almost of similar performance (AUC for RF-PR=0.749 and for SE AUC=0.745). The final conclusion of the current research was that both of the bivariate models are proficient to yield groundwater potential regions with very decent accuracy. Generally, the achievements of our current study revealed that the models examined could be applied effectively in spatial prediction modeling. The results of current study will help relevant authorities, water management, and policy makers to broadly assess GW exploration and environmental organization developments in Egypt's Suez governorate in future plans.

References:

Abd Ellah, R. G. (2020). Water resources in Egypt and their challenges, Lake Nasser case study. *Egyptian Journal of Aquatic Research*, *46*(1), 1–12. https://doi.org/10.1016/j.ejar.2020.03.001.

Abdel Samie, S. G., Elewa, H. H., Ahn, T.-K., Lee, M., Ruttan, L. M., Walker, J. M., de Ferranti, D., Perry, G. E., Foster, W., & Lederman, D. (2005). Hydrogeochemical and Environmental Isotopic Evaluation. *Egyptian Journal of Geology*, *49*, 109–131.

Abijith, D., Saravanan, S., Singh, L., Jennifer, J. J., Saranya, T., & Parthasarathy, K. S. S. (2020). GIS-based multi-criteria analysis for identification of potential groundwater recharge zones - a case study from Ponnaniyaru watershed, Tamil Nadu, India. *HydroResearch*, *3*, 1–14.

Abu El-Magd, S. A., & Eldosouky, A. M. (2021). An improved approach for predicting the groundwater potentiality in the low desert lands; El-Marashda area, Northwest Qena City, Egypt. *Journal of African Earth Sciences*, *179*, 104200. https://doi.org/10.1016/j.jafrearsci.2021.104200.

Abu El-Magd, S. A., & Embaby, A. (2021). To investigate groundwater potentiality, a GIS-based model was integrated with remote sensing data in

the Northwest Gulf of Suez (Egypt). *Arabian Journal of Geosciences*, *14*(24), 2737. https://doi.org/10.1007/s12517-021-08396-2.

Acharya, T. D., & Lee, D. H. (2019). Landslide susceptibility mapping using relative frequency and predictor rate along Araniko Highway. *KSCE Journal of Civil Engineering*, *23*(2), 763–776.

Agarwal, R., & Garg, P. K. (2016). Remote sensing and GIS based groundwater potential & recharge zones mapping using multi-criteria decision making technique. *Water Resources Management*, *30*(1), 243–260.

Ahmadi, H., Kaya, O. A., Babadagi, E., Savas, T., & Pekkan, E. (2021). GIS-Based Groundwater Potentiality Mapping Using AHP and. *Environmental Sciences Proceedings*, *2021*(5), 1–15.

Ahmed, M. A. M. (2018). *Evaluation of the Environmental System in Suez Governorate A Geographical Study using Hyper – Multi Spectral data And Geographic Information system*. Benha University (in arbic).

Akinlalu, A. A., Adegbuyiro, A., Adiat, K. A. N., Akeredolu, B. E., & Lateef, W. Y. (2017). Application of multi-criteria decision analysis in prediction of groundwater resources potential: A case of Oke-Ana, Ilesa Area Southwestern, Nigeria. *NRIAG Journal of Astronomy and Geophysics*, *6*(1), 184–200. https://doi.org/10.1016/j.nrjag.2017.03.001.

Al-Abadi, A. M., Al-Temmeme, A. A., & Al-Ghanimy, M. A. (2016). A GIS-based combining of frequency ratio and index of entropy approaches for mapping groundwater availability zones at Badra–Al Al-Gharbi–Teeb areas, Iraq. *Sustainable Water Resources Management*, *2*(3), 265–283.

Al Saud, M. (2010). Mapping potential areas for groundwater storage in Wadi Aurnah Basin, western Arabian Peninsula, using remote sensing and geographic information system techniques. *Hydrogeology Journal*, *18*(6), 1481–1495. https://doi.org/10.1007/s10040-010-0598-9.

Allafta, H., & Opp, C. (2021). GIS-based multi-criteria analysis for flood prone areas mapping in the trans-boundary Shatt Al-Arab basin, Iraq-Iran. *Geomatics, Natural Hazards and Risk*, *12*(1), 2087–2116.

Allam, A. R., Saaf, E.-J., & Dawoud, M. A. (2003). Desalination of brackish groundwater in Egypt. *Desalination*, *152*(1), 19–26. https://doi.org/https://doi.org/10.1016/S0011-9164(02)01044-5

Allam, M. N., & Allam, G. I. (2007). Water resources in Egypt: Future challeges and opportunities. *Water International*, *32*(2), 205–218. https://doi.org/10.1080/02508060708692201.

Amiri, V., Rezaei, M., & Sohrabi, N. (2014). Groundwater quality assessment using entropy weighted water quality index (EWQI) in Lenjanat, Iran. *Environmental Earth Sciences*, *72*(9), 3479–3490. https://doi.org/10.1007/s12665-014-3255-0.

Anbarasu, S., Brindha, K., & Elango, L. (2020). Multi-influencing factor method for delineation of groundwater potential zones using remote sensing and GIS techniques in the western part of Perambalur district, southern India. *Earth Science Informatics*, *13*(2), 317–332. https://doi.org/10.1007/s12145-019-00426-8.

Anbazhagan, S., & Ramasamy, S. M. (2006). Evaluation of areas for artificial groundwater recharge in Ayyar basin, Tamil Nadu, India through statistical terrain analysis. *J Geol Soci India*, *67*, 59–68.

Arabameri, A., Saha, S., Chen, W., Roy, J., Pradhan, B., & Bui, D. T. (2020).

Flash flood susceptibility modelling using functional tree and hybrid ensemble techniques. *Journal of Hydrology*, *587*, 125007.

Arshad, A., Zhang, Z., Zhang, W., & Dilawar, A. (2020). Mapping favorable groundwater potential recharge zones using a GIS-based analytical hierarchical process and probability frequency ratio model: A case study from an agro-urban region of Pakistan. *Geoscience Frontiers*, *11*(5), 1805–1819. https://doi.org/10.1016/j.gsf.2019.12.013.

Arulbalaji, P., Sreelash, K., Maya, K., & Padmalal, D. (2019). Hydrological assessment of groundwater potential zones of Cauvery River Basin, India: a geospatial approach. *Environmental Earth Sciences*, *78*(24), 1–21. https://doi.org/10.1007/s12665-019-8673-6.

Ayazi, M. H., Pirasteh, S., Arvin, A. K. P., Pradhan, B., Nikouravan, B., & Mansor, S. (2010). Disasters and risk reduction in groundwater: Zagros Mountain Southwest Iran using geoinformatics techniques. *Disaster Adv*, *3*(1), 51–57.

Bagyaraj, M., Tenaw Mengistie, A., Gnanachandrasamy, G., & Gemechu, B. (2019). Data of remote sensing and GIS - to demarcate the potential sector of groundwater in Debre Berhan, Amhara region, Ethiopia. *Data in Brief*, *26*, 104542. https://doi.org/https://doi.org/10.1016/j.dib.2019.104542.

Bednarik, M., Magulová, B., Matys, M., & Marschalko, M. (2010). Landslide susceptibility assessment of the Kraľovany–Liptovský Mikuláš railway case study. *Physics and Chemistry of the Earth, Parts A/B/C*, *35*(3–5), 162–171.

Catani, F., Lagomarsino, D., Segoni, S., & Tofani, V. (2013). Landslide susceptibility estimation by random forests technique: sensitivity and scaling issues. *Natural Hazards and Earth System Sciences*, *13*(11), 2815–2831.

Chen, L., Gao, R., Bian, Y., & Di, H. (2021). Elliptic entropy of uncertain random variables with application to portfolio selection. *Soft Computing*, *25*, 1925–1939.

Chen, W., Li, H., Hou, E., Wang, S., Wang, G., Panahi, M., Li, T., Peng, T., Guo, C., & Niu, C. (2018). GIS-based groundwater potential analysis using novel ensemble weights-of-evidence with logistic regression and functional tree models. *Science of the Total Environment*, *634*, 853–867.

Chenini, I., Mammou, A. Ben, & El May, M. (2010). Groundwater Recharge Zone Mapping Using GIS-Based Multi-criteria Analysis: A Case Study in Central Tunisia (Maknassy Basin). *Water Resources Management*, *24*(5), 921–939. https://doi.org/10.1007/s11269-009-9479-1

Chung, C.-J. F., & Fabbri, A. G. (2003). Validation of spatial prediction models for landslide hazard mapping. *Natural Hazards*, *30*(3), 451–472.

Clifton, C., Evans, R., Hayes, S., Hirji, R., Puz, G., & Pizarro, C. (2010). Water and climate change: impacts on groundwater resources and adaptation options. In *Managing* (Issue 25).

Corsini, A., Cervi, F., & Ronchetti, F. (2009). Weight of evidence and artificial neural networks for potential groundwater spring mapping: an application to the Mt. Modino area (Northern Apennines, Italy). *Geomorphology*, *111*(1–2), 79–87.

Das, S. (2019). Comparison among influencing factor, frequency ratio, and analytical hierarchy process techniques for groundwater potential zonation in Vaitarna basin, Maharashtra, India. *Groundwater for Sustainable*

Development, *8*, 617–629.

Devkota, K. C., Regmi, A. D., Pourghasemi, H. R., Yoshida, K., Pradhan, B., Ryu, I. C., Dhital, M. R., & Althuwaynee, O. F. (2013). Landslide susceptibility mapping using certainty factor, index of entropy and logistic regression models in GIS and their comparison at Mugling–Narayanghat road section in Nepal Himalaya. *Natural Hazards*, *65*(1), 135–165.

Dibaba, W. T., Demissie, T. A., & Miegel, K. (2020). Watershed hydrological response to combined land use/land cover and climate change in highland Ethiopia: Finchaa catchment. *Water*, *12*(6), 1801.

Ding, Q., Chen, W., & Hong, H. (2017). Application of frequency ratio, weights of evidence and evidential belief function models in landslide susceptibility mapping. *Geocarto International*, *32*(6), 619–639.

El-Behiry, M. G., Shedid, A., Abu-Khadra, A. O., & El-Huseiny, M. (2006). Integrated GIS and remote sensing for runoff hazard analysis in Ain Sukhna Industrial Area, Egypt. *Earth Sciences*, *17*(1).

El-Kholei, A., Abdulhamid, E., Ibrahim, G., Negm, M., & Mofty, S. (2004). *The Environmental Profile of the Governorate of Suez*.

El-Omla, M. M., & Aboulela, H. A. (2012). *Environmental and mineralogical studies of the sabkhas soil at Ismailia—Suez roadbed, southern of Suez Canal district, Egypt*. *2*(3), 165–181. https://doi.org/10.4236/ojg.2012.23017

El Osta, M. M., El Sheikh, A. El, & Barseem, M. S. (2010). Comparative hydrological and geoelectrical study on the quaternary aquifer in the deltas of Wadi Badaa and Ghweiba, El Ain El Sukhna Area, Northwest Suez Gulf, Egypt. *International Journal of Geophysics*, *2010*. https://doi.org/https://doi.org/10.1155/2010/585243.

Elbeih, S. F. (2015). An overview of integrated remote sensing and GIS for groundwater mapping in Egypt. *Ain Shams Engineering Journal*, *6*(1), 1–15.

Elmahdy, S. I., & Mohamed, M. M. (2015). Probabilistic frequency ratio model for groundwater potential mapping in Al Jaww plain, UAE. *Arabian Journal of Geosciences*, *8*(4), 2405–2416.

Ercanoglu, M., & Gokceoglu, C. (2002). Assessment of landslide susceptibility for a landslide-prone area (north of Yenice, NW Turkey) by fuzzy approach. *Environmental Geology*, *41*(6), 720–730.

Etikala, B., Golla, V., Li, P., & Renati, S. (2019). Deciphering groundwater potential zones using MIF technique and GIS: A study from Tirupati area, Chittoor District, Andhra Pradesh, India. *HydroResearch*, *1*, 1–7.

Fitts, C. R. (2012). *Groundwater science* . Elsevier. https://doi.org/https://doi.org/10.1016/C2009-0-62950-0.

Gebreyohannes, T., De Smedt, F., Walraevens, K., Gebresilassie, S., Hussien, A., Hagos, M., Amare, K., Deckers, J., & Gebrehiwot, K. (2017). Regional groundwater flow modeling of the Geba basin, northern Ethiopia. *Hydrogeology Journal*, *25*(3), 639–655. https://doi.org/10.1007/s10040-016-1522-8.

Gilani, H., Ahmad, S., Qazi, W. A., Abubakar, S. M., & Khalid, M. (2020). Monitoring of urban landscape ecology dynamics of Islamabad capital territory (ICT), Pakistan, over four decades (1976–2016). *Land*, *9*(4), 123.

Gnanachandrasamy, G., Zhou, Y., Bagyaraj, M., Venkatramanan, S., Ramkumar, T., & Wang, S. (2018). Remote sensing and GIS based groundwater potential zone mapping in Ariyalur District, Tamil Nadu. *Journal of the Geological*

Society of India, *92*(4), 484–490.

GOPP. (2014). *Environmental approach strategy for urban development in Egypt (Suez Canal region).* http://gopp.gov.eg/ (in arbic).

Guru, B., Seshan, K., & Bera, S. (2017). Frequency ratio model for groundwater potential mapping and its sustainable management in cold desert, India. *Journal of King Saud University - Science*, *29*(3), 333–347. https://doi.org/https://doi.org/10.1016/j.jksus.2016.08.003.

Hammad, M. A. (1975). Geological map of Egypt. *Appendix 1. Soil Survey Papers No. 11*.

Hefny, K., & Shata, A. (2004). Underground water in Egypt. *Ministry of Water Supplies and Irrigation, Cairo, Egypt*, *295*.

Heikal, S. A. . (2013). *Mapping Terrain Characteristic in the Northern Gulf of Suez*. zagazig.

Hou, E., Wang, J., & Chen, W. (2018). A comparative study on groundwater spring potential analysis based on statistical index, index of entropy and certainty factors models. *Geocarto International*, *33*(7), 754–769. https://doi.org/10.1080/10106049.2017.1299801

Ihara, S. (1993). *Information theory for continuous systems* (Vol. 2). World Scientific.

Jenness, J. (2006). Topographic position index (tpi_jen. avx_extension for Arcview 3. x, v. 1.3 a, Jenness Enterprises [EB/OL]. *Http://Www. Jennessent. Com/Arcview/Tpi. Htm*.

Karra, K., Kontgis, C., Statman-Weil, Z., Mazzariello, J. C., Mathis, M., & Brumby, S. P. (2021). Global land use/land cover with Sentinel 2 and deep learning. *2021 IEEE International Geoscience and Remote Sensing Symposium IGARSS*, 4704–4707.

Khan, A., Govil, H., Taloor, A. K., & Kumar, G. (2020). Identification of artificial groundwater recharge sites in parts of Yamuna River basin India based on Remote Sensing and Geographical Information System. *Groundwater for Sustainable Development*, *11*, 100415.

Khosravi, K., Sartaj, M., Tsai, F. T.-C., Singh, V. P., Kazakis, N., Melesse, A. M., Prakash, I., Bui, D. T., & Pham, B. T. (2018). A comparison study of DRASTIC methods with various objective methods for groundwater vulnerability assessment. *Science of the Total Environment*, *642*, 1032–1049.

Kim, J.-C., Jung, H.-S., & Lee, S. (2019). Spatial mapping of the groundwater potential of the geum river basin using ensemble models based on remote sensing images. *Remote Sensing*, *11*(19), 2285.

Kotchoni, D. O. V., Vouillamoz, J.-M., Lawson, F. M. A., Adjomayi, P., Boukari, M., & Taylor, R. G. (2019). Relationships between rainfall and groundwater recharge in seasonally humid Benin: a comparative analysis of long-term hydrographs in sedimentary and crystalline aquifers. *Hydrogeology Journal*, *27*(2), 447–457. https://doi.org/10.1007/s10040-018-1806-2

Lakshmi, D. S. V., & Reddy, Y. V. K. (2018). Identification of Groundwater Potential Zones Using Gis and Remote Sensing. *International Journal of Pure and Applied Mathematics*, *119*(17), 3195–3210.

Li, P., He, S., Yang, N., & Xiang, G. (2018). Groundwater quality assessment for domestic and agricultural purposes in Yan'an City, northwest China: implications to sustainable groundwater quality management on the Loess

Plateau. *Environmental Earth Sciences*, *77*(23), 1–16.

Machiwal, D., Jha, M. K., & Mal, B. C. (2011). Assessment of Groundwater Potential in a Semi-Arid Region of India Using Remote Sensing, GIS and MCDM Techniques. *Water Resources Management*, *25*(5), 1359–1386. https://doi.org/10.1007/s11269-010-9749-y.

Magesh, N. S., Chandrasekar, N., & Soundranayagam, J. P. (2012). Delineation of groundwater potential zones in Theni district, Tamil Nadu, using remote sensing, GIS and MIF techniques. *Geoscience Frontiers*, *3*(2), 189–196. https://doi.org/https://doi.org/10.1016/j.gsf.2011.10.007.

Meles, M. B., Younger, S. E., Jackson, C. R., Du, E., & Drover, D. (2020). Wetness index based on landscape position and topography (WILT): Modifying TWI to reflect landscape position. *Journal of Environmental Management*, *255*, 109863.

Mogaji, K. A., Lim, H. S., & Abdullah, K. (2015). Regional prediction of groundwater potential mapping in a multifaceted geology terrain using GIS-based Dempster–Shafer model. *Arabian Journal of Geosciences*, *8*(5), 3235–3258. https://doi.org/10.1007/s12517-014-1391-1.

Mogaji, K. A., Omosuyi, G. O., Adelusi, A. O., & Lim, H. S. (2016). Application of GIS-Based Evidential Belief Function Model to Regional Groundwater Recharge Potential Zones Mapping in Hardrock Geologic Terrain. *Environmental Processes*, *3*(1), 93–123. https://doi.org/10.1007/s40710-016-0126-6.

Moghaddam, D. D., Rezaei, M., Pourghasemi, H. R., Pourtaghie, Z. S., & Pradhan, B. (2015). Groundwater spring potential mapping using bivariate statistical model and GIS in the Taleghan Watershed, Iran. *Arabian Journal of Geosciences*, *8*(2), 913–929. https://doi.org/10.1007/s12517-013-1161-5.

Monsef, A.-E., & Smith, S. E. (2019). Integrating remote sensing, geographic information system, and analytical hierarchy process for hazardous waste landfill site selection. *Arabian Journal of Geosciences*, *12*(5), 1–14.

Mousavi, S. M., Golkarian, A., Naghibi, S. A., Kalantar, B., & Pradhan, B. (2017). GIS-based Groundwater Spring Potential Mapping Using Data Mining Boosted Regression Tree and Probabilistic Frequency Ratio Models in Iran. *AIMS Geosciences*, *3*(1), 91–115. https://doi.org/10.3934/geosci.2017.1.91

Mukherjee, I., & Singh, U. K. (2020). Delineation of groundwater potential zones in a drought-prone semi-arid region of east India using GIS and analytical hierarchical process techniques. *CATENA*, *194*, 104681. https://doi.org/https://doi.org/10.1016/j.catena.2020.104681.

Naghibi, S. A., Pourghasemi, H. R., & Dixon, B. (2015). GIS-based groundwater potential mapping using boosted regression tree, classification and regression tree, and random forest machine learning models in Iran. *Environmental Monitoring and Assessment*, *188*(1), 44. https://doi.org/10.1007/s10661-015-5049-6.

Naghibi, S. A., Pourghasemi, H. R., Pourtaghi, Z. S., & Rezaei, A. (2015). Groundwater qanat potential mapping using frequency ratio and Shannon's entropy models in the Moghan watershed, Iran. *Earth Science Informatics*, *8*(1), 171–186.

Nampak, H., Pradhan, B., & Manap, M. A. (2014). Application of GIS based data driven evidential belief function model to predict groundwater potential zonation. *Journal of Hydrology*, *513*, 283–300.

Nasir, M. J., Khan, S., Zahid, H., & Khan, A. (2018). Delineation of groundwater potential zones using GIS and multi influence factor (MIF) techniques: a study of district Swat, Khyber Pakhtunkhwa, Pakistan. *Environmental Earth Sciences*, *77*(10), 367. https://doi.org/10.1007/s12665-018-7522-3.

Nguyen, P. T., Ha, D. H., Avand, M., Jaafari, A., Nguyen, H. D., Al-Ansari, N., Van Phong, T., Sharma, R., Kumar, R., & Le, H. Van. (2020). Soft computing ensemble models based on logistic regression for groundwater potential mapping. *Applied Sciences*, *10*(7), 2469.

Oh, H.-J., Kim, Y.-S., Choi, J.-K., Park, E., & Lee, S. (2011). GIS mapping of regional probabilistic groundwater potential in the area of Pohang City, Korea. *Journal of Hydrology*, *399*(3), 158–172. https://doi.org/https://doi.org/10.1016/j.jhydrol.2010.12.027.

Osinowo, O. O., & Arowoogun, K. I. (2020). A multi-criteria decision analysis for groundwater potential evaluation in parts of Ibadan, southwestern Nigeria. *Applied Water Science*, *10*(11), 228. https://doi.org/10.1007/s13201-020-01311-2.

Perera, E. N. C., Jayawardana, D. T., Jayasinghe, P., & Ranagalage, M. (2019). Landslide vulnerability assessment based on entropy method: A case study from Kegalle district, Sri Lanka. *Modeling Earth Systems and Environment*, *5*(4), 1635–1649.

Pham, B. T., Tien Bui, D., Indra, P., & Dholakia, M. B. (2015). Landslide susceptibility assessment at a part of Uttarakhand Himalaya, India using GIS – based statistical approach of frequency ratio method. *Int. J. Eng. Res. Technol.*, *4*(11), 338–344.

Pourghasemi, H. R., Mohammady, M., & Pradhan, B. (2012). Landslide susceptibility mapping using index of entropy and conditional probability models in GIS: Safarood Basin, Iran. *Catena*, *97*, 71–84.

Pourtaghi, Z. S., & Pourghasemi, H. R. (2014). GIS-based groundwater spring potential assessment and mapping in the Birjand Township, southern Khorasan Province, Iran. *Hydrogeology Journal*, *22*(3), 643–662. https://doi.org/10.1007/s10040-013-1089-6.

Rahmati, O., Pourghasemi, H. R., & Melesse, A. M. (2016). Application of GIS-based data driven random forest and maximum entropy models for groundwater potential mapping: A case study at Mehran Region, Iran. *Catena*, *137*, 360–372. https://doi.org/10.1016/j.catena.2015.10.010

Rajabi, M., Mansourian, A., Pilesjö, P., Hedefalk, F., Groth, R., & Bazmani, A. (2014). *Comparing Knowledge-Driven and Data-Driven Modeling methods for susceptibility mapping in spatial epidemiology: a case study in Visceral Leishmaniasis*. https://repositori.uji.es/xmlui/handle/10234/98684

Rajaveni, S. P., Brindha, K., & Elango, L. (2017). Geological and geomorphological controls on groundwater occurrence in a hard rock region. *Applied Water Science*, *7*(3), 1377–1389.

Rajaveni, S. P., Brindha, K., Rajesh, R., & Elango, L. (2014). Spatial and temporal variation of groundwater level and its relation to drainage and intrusive rocks in a part of Nalgonda District, Andhra Pradesh, India. *Journal of the Indian Society of Remote Sensing*, *42*(4), 765–776.

Razandi, Y., Pourghasemi, H. R., Neisani, N. S., & Rahmati, O. (2015). Application of analytical hierarchy process, frequency ratio, and certainty

factor models for groundwater potential mapping using GIS. *Earth Science Informatics*, *8*, 867–883.

Reilly, T. E., Dennehy, K. F., Alley, W. M., & Cunningham, W. L. (2008). Ground-Water Availability in the United States. In *Circular*. https://doi.org/10.3133/cir1323.

Saeed, N. T. M., Fathi, M., & Kuhnert, K.-D. (2018). An Approach for Instant Conversion of Sensory Data of a Simulated Sensor of a Mobile Robot into Semantic Information. *IEEE International Conference on Electro Information Technology*, *2018-May*, 142–146. https://doi.org/10.1109/EIT.2018.8500087.

Saha, D., Dhar, Y. R., & Vittala, S. S. (2010). Delineation of groundwater development potential zones in parts of marginal Ganga Alluvial Plain in South Bihar, Eastern India. *Environmental Monitoring and Assessment*, *165*(1–4), 179–191. https://doi.org/10.1007/s10661-009-0937-2.

Salim, M. G. (2012). Selection of groundwater sites in Egypt, using geographic information systems, for desalination by solar energy in order to reduce greenhouse gases. *Journal of Advanced Research*, *3*(1), 11–19.

Sar, N., Khan, A., Chatterjee, S., & Das, A. (2015). Hydrologic delineation of ground water potential zones using geospatial technique for Keleghai river basin, India. *Modeling Earth Systems and Environment*, *1*(3), 1–15.

Selvam, S., Dar, F. A., Magesh, N. S., Singaraja, C., Venkatramanan, S., & Chung, S. Y. (2016). Application of remote sensing and GIS for delineating groundwater recharge potential zones of Kovilpatti Municipality, Tamil Nadu using IF technique. *Earth Science Informatics*, *9*(2), 137–150. https://doi.org/10.1007/s12145-015-0242-2

Selvam, S., Manimaran, G., Sivasubramanian, P., & Seshunarayana, T. (2014). Geoenvironmental esource Assessment Using Remote Sensing and GIS: A case study from southern coastal region. *Research Journal of Recent Sciences*, *3*(1), 108–115. https://www.scopus.com/inward/record.uri?eid=2-s2.0-84899837560&partnerID=40&md5=ae96cbdd84b213b24a7b858513596e7f.

Shahid, S., & Hazarika, M. K. (2010). Groundwater drought in the northwestern districts of Bangladesh. *Water Resources Management*, *24*(10), 1989–2006. https://doi.org/10.1007/s11269-009-9534-y.

Shahinuzzaman, M., Haque, M. N., & Shahid, S. (2021). Delineation of groundwater potential zones using a parsimonious concept based on catastrophe theory and analytical hierarchy process. *Hydrogeology Journal*, *29*(3), 1091–1116. https://doi.org/10.1007/s10040-021-02322-2.

Shekhar, S., & Pandey, A. C. (2015). Delineation of groundwater potential zone in hard rock terrain of India using remote sensing, geographical information system (GIS) and analytic hierarchy process (AHP) techniques. *Geocarto International*, *30*(4), 402–421. https://doi.org/10.1080/10106049.2014.894584.

Singh, P., Thakur, J. K., & Kumar, S. (2013). Delineating groundwater potential zones in a hard-rock terrain using geospatial tool. *Hydrological Sciences Journal*, *58*(1), 213–223.

Snousy, M. G., Zawrah, M. F., Abdel-Moghny, T., Ebiad, M. A., Rashad, A. M., Khalil, M. M., Abu El Ella, E. M., El-Sayed, E., & Tantawy, M. A. (2016). *Mobility and Fate of Pollutants in the Aquifer System of the Northwestern*

Suez Gulf, Egypt BT - Reviews of Environmental Contamination and Toxicology Volume 240 (P. de Voogt (ed.); pp. 169–195). Springer International Publishing. https://doi.org/10.1007/398_2016_5.

Solomon, S., & Quiel, F. (2006a). Groundwater study using remote sensing and geographic information systems (GIS) in the central highlands of Eritrea. *Hydrogeology Journal*, *14*(5), 729–741. https://doi.org/10.1007/s10040-005-0477-y.

Solomon, S., & Quiel, F. (2006b). Groundwater study using remote sensing and geographic information systems (GIS) in the central highlands of Eritrea. *Hydrogeology Journal*, *14*(6), 1029–1041. https://doi.org/10.1007/s10040-006-0096-2.

Srivastava, V. K., Giri, D. N., & Bharadwaj, P. (2012). Study and Mapping of Ground Water Prospect using Remote Sensing, GIS and Geoelectrical resistivity techniques-a case study of Dhanbad district, Jharkhand, India. *J. Ind. Geophys. Union*, *16*(2), 55–63.

Sun, J., He, F., Zhang, Z., Shao, H., Pan, Y., Yang, R., Li, W., Li, P., & Zheng, M. (2018). Analysis of saline groundwater infiltration into two loam soils. *Land Degradation and Development*, *29*(10), 3795–3802.

Swets, J. A. (1988). Measuring the accuracy of diagnostic systems. *Science*, *240*(4857), 1285–1293.

Taha, A. E. H. A., El Mahmoudi, A. S., & El-Haddad, I. M. (2005). Geoelectrical exploration for groundwater around the new communities, East Nile Delta. *Proceedings of the Symposium on the Application of Geophyics to Engineering and Environmental Problems, SAGEEP*, *1*(January 2005), 498–514. https://doi.org/10.4133/1.2923517

Thapa, R., Gupta, S., Gupta, A., Reddy, D. V, & Kaur, H. (2018). Use of geospatial technology for delineating groundwater potential zones with an emphasis on water-table analysis in Dwarka River basin, Birbhum, India. *Hydrogeology Journal*, *26*(3), 899–922. https://doi.org/10.1007/s10040-017-1683-0.

Thapa, R., Gupta, S., & Kaur, H. (2017). Delineation of potential fluoride contamination zones in Birbhum, West Bengal, India, using remote sensing and GIS techniques. *Arabian Journal of Geosciences*, *10*(23), 1–18. https://doi.org/10.1007/s12517-017-3328-y.

Trabelsi, F., Lee, S., Khlifi, S., & Arfaoui, A. (2019). *Frequency Ratio Model for Mapping Groundwater Potential Zones Using GIS and Remote Sensing; Medjerda Watershed Tunisia BT - Advances in Sustainable and Environmental Hydrology, Hydrogeology, Hydrochemistry and Water Resources* (H. I. Chaminé, M. Barbieri, O. Kisi, M. Chen, & B. J. Merkel (eds.); pp. 341–345). Springer International Publishing.

U.N, W. (2018). Sustainable Development Goal 6 Synthesis Report on Water and Sanitation 2018. In *United Nations New York: New York, NY, USA*.

Waikar, M. L., & Nilawar, A. P. (2014). Morphometric Analysis of a Drainage Basin Using Geographical Information System : A Case study. *International Journal of Multidisciplinary and Current Research*, *2*(2014), 179–184.

Wan, S. (2009). A spatial decision support system for extracting the core factors and thresholds for landslide susceptibility map. *Engineering Geology*, *108*(3–4), 237–251.

Wang, J., Zhou, Y., & Xiao, F. (2020). Identification of multi-element geochemical anomalies using unsupervised machine learning algorithms: A case study from Ag–Pb–Zn deposits in north-western Zhejiang, China. *Applied Geochemistry*, *120*, 104679.

Water, U. N. (2015). *World Water Development Report: Water for a sustainable world*. http://www.unesco.org/new/en/naturalsciences/environment/water/wwap/wwdr/2015-water-for-a-sustainable-world/

Weiss, A. (2001). Topographic position and landforms analysis. *Poster Presentation, ESRI User Conference, San Diego, CA*, *200*.

World Health Organization. (2010). *UN-water global annual assessment of sanitation and drinking-water : GLAAS 2010 : targeting resources for better results.* World Health Organization.

Yariyan, P., Avand, M., Abbaspour, R. A., Torabi Haghighi, A., Costache, R., Ghorbanzadeh, O., Janizadeh, S., & Blaschke, T. (2020). Flood susceptibility mapping using an improved analytic network process with statistical models. *Geomatics, Natural Hazards and Risk*, *11*(1), 2282–2314.

Yesilnacar, E., & Topal, T. (2005). Landslide susceptibility mapping: a comparison of logistic regression and neural networks methods in a medium scale study, Hendek region (Turkey). *Engineering Geology*, *79*(3–4), 251–266.

Yifru, B. A., Chung, I.-M., Kim, M.-G., & Chang, S. W. (2021). Assessing the effect of land/use land cover and climate change on water yield and groundwater recharge in East African Rift Valley using integrated model. *Journal of Hydrology: Regional Studies*, *37*, 100926.

Youssef, A. M., Pradhan, B., & Tarabees, E. (2011). Integrated evaluation of urban development suitability based on remote sensing and GIS techniques: contribution from the analytic hierarchy process. *Arabian Journal of Geosciences*, *4*(3), 463–473. https://doi.org/10.1007/s12517-009-0118-1

Zabihi, M., Pourghasemi, H., & Behzadfar, M. (2015). Groundwater Potential Mapping using Shannon's Entropy and Random Forest Models in the Bojnourd Plain. *Ecohydrology*, *2*, 221–232.

Zaghlol, S., Wahid, A., & Mahfouz, N. (2016). Determination of Favorable Sites for Wind Farm Constructions Using Remote Sensing and Geographic Information Systems (GIS) in Suez Governorate, Egypt. *Tectonophysics*, *153*(1–4), 249–270.

Zandi, J., Ghazvinei, P. T., Hashim, R., Yusof, K. B. W., Ariffin, J., & Motamedi, S. (2016). Mapping of regional potential groundwater springs using Logistic Regression statistical method. *Water Resources*, *43*(1), 48–57. https://doi.org/10.1134/S0097807816010097

Zhou, S., Zhou, S., & Tan, X. (2020). Nationwide susceptibility mapping of landslides in Kenya using the fuzzy analytic hierarchy process model. *Land*, *9*(12), 1–22. https://doi.org/10.3390/land9120535

Zomlot, Z., Verbeiren, B., Huysmans, M., & Batelaan, O. (2017). Trajectory analysis of land use and land cover maps to improve spatial–temporal patterns, and impact assessment on groundwater recharge. *Journal of Hydrology*, *554*, 558–569.